THESIS FOR THE DEGREE OF LICENTIATE OF ENGINEERING

Energy Performance and Manoeuvring Modelling of Inland Waterway Vessels

CHENGQIAN ZHANG

Department of Mechanics and Maritime Sciences
CHALMERS UNIVERSITY OF TECHNOLOGY
Gothenburg, Sweden 2023

Energy Performance and Manoeuvring Modelling of Inland Waterway Vessels

CHENGQIAN ZHANG

Report No 2023:17

Chalmers University of Technology
Department of Mechanics and Maritime Sciences
Division of Marine Technology
SE-412 96, Gothenburg
Sweden
Telephone: + 46 (0)31-772 1000

Printed by Chalmers Reproservice
Gothenburg, Sweden 2023

Energy Performance and Manoeuvring Modelling of Inland Waterway Vessels

CHENGQIAN ZHANG
Chalmers University of Technology
Department of Mechanics and Maritime Sciences
Division of Marine Technology

Abstract

Inland waterway transport has significant potential to reduce greenhouse emissions and road congestion safely and sustainably. To construct competitive, intelligent waterborne transport networks, the use of advanced vessels with clean energy and a high degree of automation or autonomy is an ideal solution for next-generation transport. However, to promote the production and implementation of these autonomous inland vessels, numerous issues must be considered from both the technical and legislative perspectives. A comprehensive analysis of ship design, perception, path planning, motion control, and potential social-technical, economic, and legal issues is required.

This thesis addresses a critical issue for future autonomous vessels: energy-efficient path planning. It includes the development of an energy performance prediction model, a manoeuvring model, and an integrated voyage planning tool for energy optimisation. Research on ship resistance, propulsion, and manoeuvring has been conducted actively in recent decades. However, most methods have been developed for sea-going vessels, whose hull form and navigational conditions are distinct from those of inland ships. Only a few studies analyse the inland waterway's hydrodynamic impact, especially in restricted waterways. However, these model tests or numerical simulations usually focus on a specific issue or ship type, and holistic models for general application to these inland vessels are lacking. Therefore, this thesis aims to develop generic models that capture ship energy consumption and manoeuvring performance, specifically for inland vessels.

The thesis presents the development of an integrated ship energy system model. The model is based on a ship performance model, ShipCLEAN, with significant modifications in ship resistance prediction and propeller modelling on shallow water to capture the characteristics of inland waterway vessels (IWVs). A verification study shows that the proposed model has very good accuracy in terms of resistance and power prediction in varying water depths based solely on empirical methods. A new manoeuvring model based on the MMG model is proposed, including shallow water correction and additional bank effects on confined waterways. Turning circle tests on a pusher–barge system indicate that the proposed model can capture the vessel's steering behaviour. Then, a rudder controller is developed to analyse the rudder capacity in course keeping on confined channels with shallow water, river currents, and bank effects.

The proposed models generate fast and accurate predictions on energy consumption and dynamic motions of IWVs, with good applicability for integration into energy-efficient path planning with route algorithms and optimisation techniques.

Keywords: autonomous vessels, confinement effect, energy efficiency, inland waterways, manoeuvring prediction, ship hydrodynamics

Preface

This thesis comprises research performed starting in March 2022 at the Division of Marine Technology, Department of Mechanics and Maritime Sciences at the Chalmers University of Technology in Sweden. The EU project ETN AUTOBarge (European training and research network on Autonomous Barges for Smart Inland Shipping) provided financial support for this research through the European Union's EU Framework Programme for Research and Innovation Horizon 2020 under Grant Agreement No. 955768.

First and most importantly, I would like to express my appreciation to my main supervisor, Professor Jonas Ringsberg. Thank you for your endless support, guidance, and excellent discussions whenever I got stuck.

I would also like to thank my co-supervisors, Professor Wengang Mao, for all your nice suggestions for figuring out the direction of my research, and Dr Fabian Thies, for the many fruitful discussions and instructions from your side. I also want to thank Professor Rudy Negenborn for hosting me on a fantastic journey at TU Delft.

Thank you to all my friends and colleagues at the Division of Marine Technology and AUTOBarge project. I especially want to thank my dear friend Yucong Ma for all the joyful chats and collaborations.

Finally, I would like to express my sincerest gratitude to my beloved wife, Xue, for being the best part of my life. Words cannot express my feelings of appreciation for every single moment with you. Your support, devotion, and encouragement give me the strongest power to move forward.

Chengqian Zhang
Gothenburg, December 2023

Contents

List of appended papers

Paper I Zhang C, Ringsberg JW, Thies F. 2023. Development of a ship performance model for power estimation of inland waterway vessels. *Ocean Engineering*. 287:115731. https://doi.org/10.1016/j.oceaneng.2023.115731.

Paper II Zhang, C., Ma, Y., Thies, F., Ringsberg, J.W., Xing, Y. 2023. Towards autonomous inland shipping: a manoeuvring model in confined waterways. Under review in *Ships and Offshore Structures.*

Nomenclature

Greek notations

α_H	Rudder force increase factor [-]
β	Drift angle at midship [rad]
β_P	Inflow angle to rudder during manoeuvring [rad]
δ	Rudder angle [deg]
ε	Ratio of wake fraction at rudder to propeller [-]
η_H	Hull efficiency [-]
η_o	Propeller open water efficiency [-]
η_R	Relative rotative efficiency [-]
η_s	Shaft transmission efficiency [-]
Λ	Rudder aspect ratio [-]
ρ_{FW}	Fresh water density [kg/m^3]
ρ_{SW}	Sea water density [kg/m^3]
τ	Propeller thrust ratio [-]
ψ	Ship heading angle [deg]

Latin notations

A_R	Rudder area [m^2]
A_{WP}	Ship waterplane area [m^2]
B	Ship beam [m]
C	Duct chord length [m]
C_B	Block coefficient [-]
C_F	Frictional resistance coefficient [-]
C_W	Wave resistance coefficient [-]
D_P	Propeller diameter [m]
d	Distance between vessel and bank [m]
Fr	Froude number [-]
Fr_h	Depth Froude number [-]
Fr_{hd}	Depth Froude number (deep water) [-]
H	Water depth [m]
K_T	Propeller thrust coefficient [-]
k	Ship form factor [-]
L	Ship length overall [m]
n	Propeller revolution speed [r/min]
n_{Prop}	Number of propellers [-]
P_D	Delivered power [kW]
P_E	Effective power [kW]

P_S	Service power [kW]
P_{max}	Engine limits [kW]
R_{AW}	Added wave resistance [kN]
R_{BANK}	Bank-induced resistance [kN]
R_s	Squat-induced resistance [kN]
R_T	Total resistance [kN]
R_W	Wind resistance [kN]
SFOC	Specific fuel oil consumption [g/kWh]
S_W	Wetted surface area [m^2]
s	Propeller slip ratio [-]
T	Ship draught [m]
t	Thrust deduction factor [-]
U	Ship speed [m/s]
U_C	River current speed [m/s]
U_R	Total inflow speed at rudder [m/s]
u	Longitudinal ship speed [m/s]
u_R	Longitudinal rudder inflow speed[m/s]
v	Lateral ship speed at centre of gravity [m/s]
v_R	Lateral rudder inflow speed [m/s]
w_E	Effective wake [-]
w_P	Wake fraction at propeller [-]
w_R	Wake fraction at rudder [-]
X_B, X_H, X_P, X_R	Surge force components from bank effect, ship hull, propellers, and rudders [kN]
Y_B, Y_H, Y_R	Sway force components from bank effect, ship hull, and rudders [kN]
y_{infl}	Influence distance of bank effect [m]

Abbreviations

CFD	Computational fluid dynamics
CoG	Centre of gravity
DoF	Degree of freedom
ETA	Estimated time of arrival [h]
IWV	Inland waterway vessel
UKC	Under keel clearance [m]

1 Introduction

This chapter starts by introducing the background of this thesis, followed by a literature review on methods for predicting ship energy performance, manoeuvring, and control techniques. Subsequently, the aims and objectives are presented, along with the study's scope, assumptions, and limitations.

1.1 Background

The European inland waterways, comprising over 41,000 kilometres of rivers and canals, form a complex transport network that connects 25 countries, hundreds of cities, and critical industrial regions. Nevertheless, these resources have remained underused during the past decade and account for only 6% of European inland freight transport (see Figure 1), in contrast to the 77% dominated by road transport. According to the Paris Agreement, the EU set a long-term strategy to be climate-neutral by 2050, with a 2030 target of 55% CO_2 emission reduction (European Commission, 2018). To reach these goals, practical solutions must be implemented to reduce greenhouse gas emissions, of which the transport sector (especially the road-based portion) contributes significantly. Considering the strict regulations on emissions and congestion problems on roads, increasing the utilisation of inland waterways can be a reliable and effective solution. Regarding CO_2 emissions per tonne-km of goods carried, inland waterway transport is one of Europe's most CO_2-efficient modes of transport (see Figure 2).

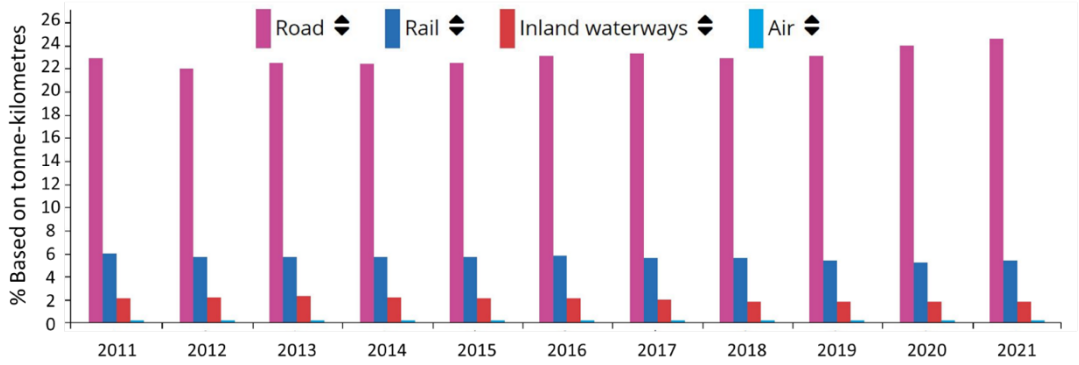

Figure 1. Freight transport by sector (European Commission, 2023).

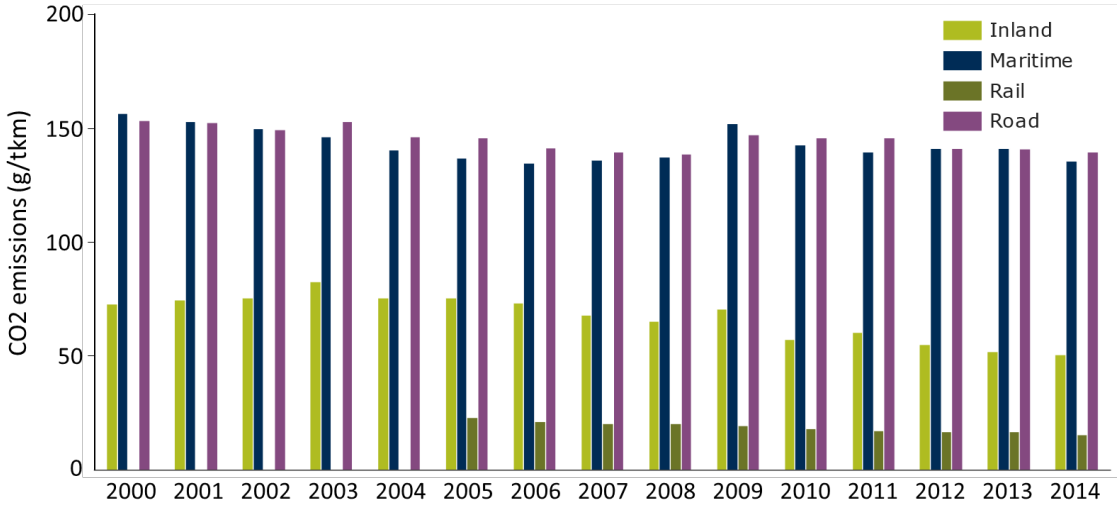

Figure 2. Specific CO_2 emissions per tonne-km by transport mode in Europe (European Environment Agency, 2017).

The increased utilisation of inland waterways should, however, be strategically planned to cater to future expectations and demands for sustainable, efficient, and dependable modes of transport. Fossil-free transport alternatives are prospective solutions characterised by a high degree of automation or autonomy. In this context, the EU project AUTOBarge (https://etn-autobarge.eu/) aims to develop an intelligent waterborne transport network by employing autonomous inland vessels, specifically barges, to enhance the reliability and sustainability of shipping from technical, economic, and legal perspectives (see Figure 3).

The second work package, Effective Path Planning and Motion Control, involves several issues, including safety concerns and considerations related to operational efficiency, which must be adequately addressed before implementing these autonomous vessels. This requires a comprehensive examination and analysis of ships' hydrodynamic behaviour, propulsion systems, manoeuvrability, and control design, given that inland vessels operate in a distinct environment compared to sea-going ships. Factors such as shallow water, channel banks, and river currents may significantly affect the vessel's navigation performance.

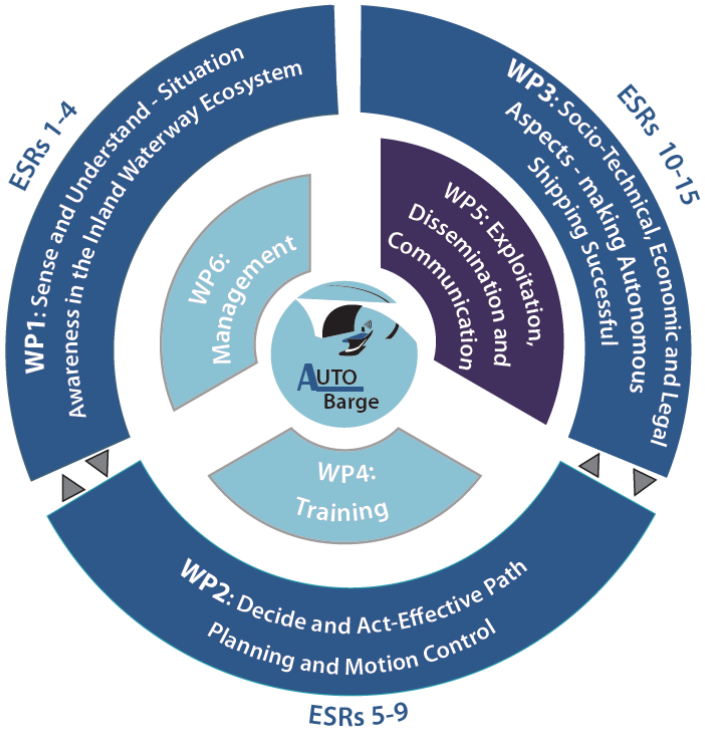

Figure 3. AUTOBarge project work packages (European Commission, 2020).

1.2 Literature review

1.2.1 Ship energy system modelling

The ship energy performance model plays a crucial role in vessels' operations. The model can capture the consumption of the energy system through the analysis of interactions among ship speed, hull resistance, propeller, engine, and dynamic waterway conditions, commonly referred to as the speed–power relationship. The categories of ship performance models can be divided into two groups: (i) white box models, primarily based on empirical or analytical methods, and (ii) black box models, constructed using data-driven methods from field-collected data or measurements.

Regarding the white box methods, a representative model named Ship Impact Model (SIM) was firstly proposed by Calleya (2014), which aimed to generate fast predictions of energy performance for commercial sea-going ships and the evaluation of different possible techniques to help reduce carbon emissions during the early design stage. Mermiris et al. (2011) proposed a dynamic energy model by integrating all the individual components of the entire ship energy system, such as the propulsion, fuel oil, ballast, and electric power system, to formulate a complex Simulink-based model. In this way, the energy flow could be predicted as a function of time for dynamic analysis of the ship's energy efficiency and cost-effectiveness during different stages (either the early design or operational phase with collected data). In addition, Lu et al. (2015) proposed a semi-empirical model for predicting a ship's fuel consumption under various loading conditions, speeds, and encountered sea states. The model was verified using a commercial ship, indicating its capability to be used for voyage optimisation. Tillig et al. (2017) developed a physically similar but more sophisticated ship energy system model based purely on empirical methods. Its critical components, such as the hull profile, resistance calculation, propeller design, and engine model, were built using a modular architecture. They can be easily modified and replaced according to the available data from the design stage to real operating analysis. Huang et al. (2021) also proposed a physics-based ship performance model specifically focusing on ice resistance prediction and energy optimisation for Arctic navigation.

Beyond the empirical formula-based models mentioned, active research has recently been conducted on data-driven methods for predicting ship energy consumption. With ample sensor measurements from various ship types and journeys, regression models are constructed for predicting power and energy consumption based on the input of ship speeds, engine loads, and environmental conditions (wind, waves, and ocean currents). Hu et al. (2019) proposed a machine learning (ML) method to predict the fuel consumption of a container ship while considering environmental factors. Parkes et al. (2018) presented an ML-based architecture on measured data from three merchant ships to formulate the relationship between shaft power and sea conditions. They also discussed the selection of neural network structures to determine the quality and quantity of data needed for accurate predictions. With the statistical analysis and appropriate data pre-processing, these data-driven models demonstrated good generalisation ability using full-scale trial data, making them effective tools for optimising a ship's operational energy efficiency (Bui & Perera, 2021; Karagiannidis & Themelis, 2021; Lang et al., 2022).

Based on the existing research, numerous ship performance models are available and have proven effective for vessels navigating open waters. Nevertheless, when shifting to applications on inland waters, the ship design, propulsion, steering devices, and, most importantly, the waterway conditions differ remarkably from sea-going vessels. Navigation and manoeuvring are challenging for inland ships due to the physics of inland waterways, such as the restricted operational space, water levels, and dynamic traffic. Consequently, models tailored to open water conditions become less applicable on rivers and canals, as they neglect the effects of shallow water and confinement, focusing instead on the influence of winds and ocean waves. Such factors are less critical to inland water transport.

When a vessel sails on the river, the reduced water level, especially during the dry season, can have a significant impact on the ship's hydrodynamic behaviour. The diminishing under-keel clearance (UKC) changes the flow around the vessel, making it prone to sinkage and trim due to the pressure difference caused by the accelerated water (see Figure 4). This results in additional resistance acting on the hull, affecting the required propulsion power and overall energy. Therefore, accurate methods for calculating the shallow water resistance and propeller–hull interactions are crucial for energy consumption prediction and the engine's operational optimisation. Empirical equations are straightforward methods derived from vast experimental data. In

terms of shallow water resistance prediction, several empirical methods have been mentioned in the literature (Aztjushkov, 1968; Geerts et al., 2010; Karpov, 1946; Lackenby, 1963; Landweber, 1939; Schlichting, 1934). These are easy to implement and can generate fast predictions of the additional resistance in shallow water. However, research by Raven (2012, 2016) has indicated that these methods have significant shortcomings when applied to inland water scenarios. First, the formulas were derived from experimental data from commercial vessels with a distinctive hull shape compared to inland ships. Moreover, the speed corrections used in these methods can oversimplify the problem in inland waterways, as the individual parts of the resistance (viscous and wave) should be carefully investigated, and the additional sinkage in shallow water must also be included (Raven, 2016).

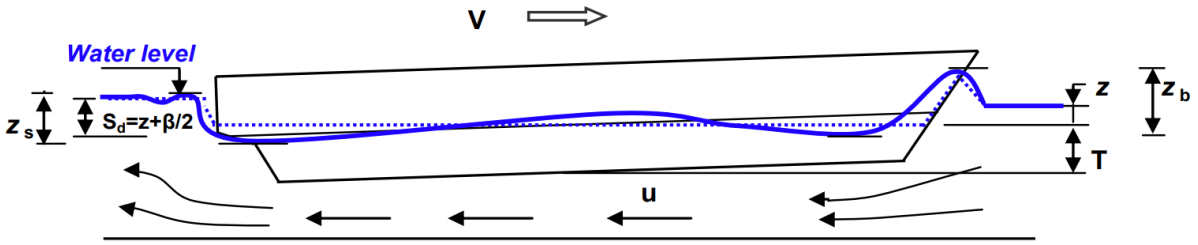

Figure 4. Scheme for shallow water effect (Pompée, 2015). The ship is subject to bow wave (Z_b) and trim β when it sails at speed V in shallow water, resulting in a dynamic squat S_d and return current u.

Model tests have been conducted over the past few years to improve prediction methods for inland vessels (Friedhoff et al., 2019; Mucha et al., 2017, 2018; Zeng et al., 2018). In addition to studies of self-propulsion vessels, Zentari et al. (2022, 2023) proposed a systematic model test with a particular focus on the resistance of pusher–barge convoys and the impact of gap flow on the vessel's hydrodynamics. Numerical simulations are another efficient method to investigate the hydrodynamics of these inland vessels on shallow or restricted waterways. Computational fluid dynamics (CFD) studies have been actively conducted during the past decade on both self-propelled vessels (Islam et al., 2021; Linde et al., 2017; Zeng et al., 2019, 2020) and pusher–barge systems (Du et al., 2020; Zentari et al., 2022). With sophisticated turbulence models and increasing computing power, CFD simulations show very good accuracy and agree well with experimental measurements.

In general, the currently available studies focus on specific hydrodynamic analysis, such as the resistance or trim prediction of a particular ship type, rather than developing generic or holistic models to reflect the performance of the entire energy system of inland waterway vessels (IWVs). Despite the accuracy of model tests or high-fidelity CFD simulations, these methods can only analyse a single operational condition, such as a constant ship speed or water level, for a specific ship model during every trial or simulation. Considering the dynamic conditions (arbitrarily shaped waterway cross sections, varying water depth and ship–bank distances, and operational speed range) of actual inland waterway transport, the solution requires a massive number of tests and simulations to cover these parameters for different hull shapes and generate such a regression model, which can be extremely expensive and time-consuming. To address this gap, the research presented in this thesis developed a holistic energy performance model, discussed in Paper I, where the components of an IWV's energy system were constructed using individual modules. The model focuses on analysing the flow and interactions between these modules to generate a detailed simulation of the overall energy consumption, which can be used for the generic operational analysis of IWVs.

1.2.2 Manoeuvring prediction

The theory of ship manoeuvring was established decades ago. An accurate manoeuvring model plays a crucial role in ensuring navigation safety, especially for ships operating on conjunctive waterways. Most existing research has focused on standard seagoing ships on open water (Abkowitz, 1964; Inoue et al., 1981; Nomoto et al., 1957; Sutulo & Soares, 2014; Yasukawa & Yoshimura, 2015). In contrast, relatively few studies have focused on ships manoeuvring on inland waterways. Compared to open water, vessels on inland waterways are subject to more complex scenarios, including water depth and channel width restrictions, dynamic traffic, and river bends. Given that IWVs will inevitably operate on these restricted waterways, an effective method to predict ship motion accurately in such complicated environments is essential to ensure safe operation.

Water level, especially the shallow water effect, can significantly affect ships' manoeuvring predictions (Kijima & Nakiri, 1990; Liu et al., 2015; Mucha et al., 2019; Yoshimura, 1986). Pompée (2015) indicated that the shallow water effect occurs if the water depth (H) is below four times the ship draught (T), while Vantorre (2003) clarified that the ship will be subject to noticeable shallow water effect if the ratio $H/T < 3.0$. A decreased water level changes the flow fields around the ship, generating additional hydrodynamic forces from the longitudinal and transversal directions. Meanwhile, under shallow water conditions, a ship's manoeuvrability also depends on its category (Liu et al., 2015). For conventional vessels with single or twin propellers, turning behaviour typically worsens with decreasing water depth. However, wide-beam ships show the inverse result, meaning they have even better turning ability in shallow water than in deep water due to the additional increment of rudder force and moment (Koh & Yasukawa, 2012; Yoshimura, 1986). This provides insight for the manoeuvring study of IWVs in that, unlike the mathematical models for conventional ships on open water, the manoeuvring model for inland vessels should include the shallow water effect and careful consideration of vessel type and steering device configuration.

In addition to shallow water restrictions, IWVs also constantly navigate narrow fairways. According to instructions from the Dutch Ministry of Infrastructure and Water Management, the minimum channel width can be two times the ship's beam for a single lane and three times for a narrow-double lane (Rijkswaterstaat, 2020). Therefore, when vessels pass each other or proceed to overtake other vessels within confined waterways, or pass through artificial river structures, such as locks, bridge pillars, and terminals, a good level of manoeuvrability is necessary for course keeping. However, research has indicated that the decreased ship–bank distance can result in a pressure difference between the portside and starboard. The riverbank can generate an additional force and moment acting on the hull, which might affect the ship's manoeuvrability and course stability, also known as the bank effect (Mucha et al., 2018; Vantorre et al., 2003; Vantorre et al., 2017; Zou & Larsson, 2013).

So far, manoeuvring studies for inland vessels have primarily focused on analysing the vessels' turning behaviour at various water depths or measuring the bank-induced force using model tests. Very few studies have aimed to propose a suitable manoeuvring model that can be applied generically to inland transport. Liu et al. (2017) made the only existing proposal, namely an integrated manoeuvring model for inland vessels with different propeller–rudder configurations. This model combined several empirical methods for calculating the hydrodynamic coefficients, predicting propulsive factors, and using CFD simulations for rudder modelling. It was tested using two typical inland vessels on the Yangtze River. However, the channel dimensions of the Yangtze River are commonly deeper and wider than the major European inland waterways. In their original model, Liu et al. (2017) did not include the effect of either water depth or bank effect, and the profile of the reference ships differs from that of European inland vessels.

In summary, the issues mentioned above indicate the remaining gap in the existing ship-manoeuvring research, namely that a suitable mathematical model has yet to be developed for application to generic inland vessels.

1.3 Objective and goals

This thesis uses an energy efficiency perspective to build an integrated model for IWVs to simulate and optimise vessels' energy consumption. Such a model should include methods for energy consumption monitoring, manoeuvring modelling, and energy-efficient route/voyage planning. This thesis primarily focuses on developing energy performance and manoeuvring models.

The main objective can be divided into several goals:

(i) Develop a holistic ship energy performance model for IWVs that captures power demand and energy consumption.
(ii) Investigate and quantify the impact of shallow water and channel width on energy consumption.
(iii) Propose a specific manoeuvring model for restricted waterways, including the hydrodynamic effects of decreasing water depth and channel banks.
(iv) Implement a rudder controller for course keeping in confined waterways.
(v) Ensure the model is based on a few ship parameters, is rapid to use in simulations, and is 'computation efficient' but still accurate in predictions.

1.4 Scope and limitations

This subchapter clarifies the assumptions and limitations of the model development methods.

Development of ship energy performance model

The model was designed for conventional vessels – such as tankers, container ships, self-propelled barges, and pusher–barge convoys – operating on European inland waterways. The model only considers ship hull longitudinal force (resistance); it neglects transversal forces and moments, as these have a minor impact on the overall propulsion power.

For resistance prediction, the model utilised a combination of empirical methods in shallow water with an applicable range of $H/T \geq 1.2$ (where H is water depth and T is vessel draught). Bank-induced resistance was modelled using a regression curve based on a selection of experimental and simulation results from the literature, with a minimum ship–bank distance of 1.0 beam.

The propeller and engine design follow the traditional configuration of IWVs, including screw and ducted propellers and classical diesel engines. Equipment such as azimuth thrusters and waterjets were not included in this model.

Manoeuvring derivation and control simulation

The manoeuvring model was developed for inland vessels with a twin-propeller twin-rudder (TPTR) configuration. The model analyses two-dimensional (2D) planar ship motion in three degrees of freedom (3-DoF), including only surge, sway, and yaw motion. The propeller force and rudder normal force were considered identical on each side, meaning that the asymmetrical flow during vessel steering was neglected for model simplification.

All simulations were conducted in a straight waterway channel with a rectangular cross-section. The river current was included in the upstream and downstream directions, with a maximum flow speed of 0.5 m/s at the waterway centreline. Forces and moments were assumed to act at the ship's centre of gravity (CoG), indicating that the simulation did not consider local speeds at different vessel locations. Regarding rudder control, a proportional-derivative (PD) controller was developed for the ship's course-keeping simulation, with a maximum rudder angle of 45°.

1.5 Thesis outline

The remainder of this thesis is divided as follows: Chapter 2 presents the methodology used to develop the ship energy performance and manoeuvring models. The applicability and parameters are also discussed in this chapter. Chapter 3 summarises the main findings and results of the selected publications. Chapter 4 presents the conclusions and Chapter 5 the insights for future work.

2 Methodology

This chapter presents the methods used for developing (i) a holistic energy system model for inland waterway vessels (IWVs) concerning power prediction and estimation of fuel consumption, (ii) a new manoeuvring model for IWVs, including hydrodynamic effects on confined waterways, and (iii) control design for rudder systems. The research related to the appended papers is indicated in the red box in Figure 5. Paper I focuses on developing the holistic ship energy performance model, and Paper II presents the manoeuvring and control modelling on confined waterways. The green box denotes future work on model integration and optimisation of voyage planning and energy management, detailed in Chapter 5 of this thesis.

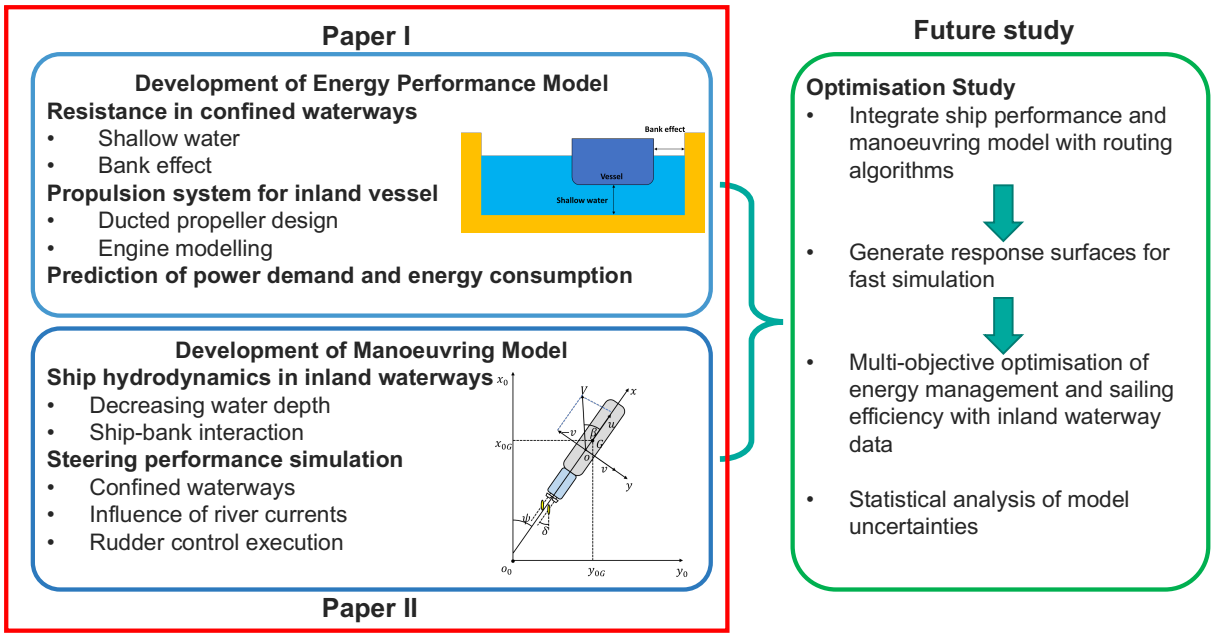

Figure 5. The outline of the work presented in this thesis.

2.1 Holistic ship energy system model

A holistic ship energy system model provides a systematic approach to analysing and monitoring energy consumption by investigating the flow and interactions between individual components and ship systems. It comprises hull geometry estimation, superstructure design and air drag prediction, resistance calculation, propeller design, and engine modelling. Tillig et al. (2017) proposed a holistic model named ShipCLEAN to analyse the energy performance of standard commercial vessels. In this model, each module represents an individual component of the entire ship's energy system. One of this model's key advantages is the flexibility of its modular architecture, as every component can be modified and extended. Newly developed modules can be incorporated during various stages, from early design to final operational analysis. Continuous development can be found in Tillig et al. (2018), Tillig and Ringsberg (2019), and Tillig (2020), where even ship retrofitting, such as wind-assisted propulsion units, can be incorporated with cost–benefit analysis based on ship type, route, and metocean data.

Considering that the ShipCLEAN model was initially designed for conventional sea-going vessels, the empirical methods selected were based on open water, and the influences of confined waterways were not included. Many existing studies have uncovered the significant influence of restricted waterways on ships' resistance, propulsion, and power prediction (Kulczyk, 1995; Kulczyk & Tabaczek, 2014; Mucha et al., 2018; Raven, 2016), and such effects must be included in the energy model for IWVs. In addition, inland vessels have a distinctive design, with

notably different hull shapes and propeller–rudder configurations – such as ducted propellers and multiple rudders – compared to sea-going ships. These factors also play an essential role in the demanded power prediction (Friedhoff et al., 2019; Kulczyk & Tabaczek, 2014), directly affecting the final energy consumption calculation. Therefore, owing to its flexible modular structure, the original ShipCLEAN model was used as the basis for a new model for inland vessel applications, ShipCLEAN-IWV. This involved significant improvements and modifications, incorporating inland waterway characteristics, and considering the unique features of inland vessels. This subchapter discusses the main methods and equations used to develop ShipCLEAN-IWV.

Figure 6 shows the architecture of the new ShipCLEAN-IWV model. The critical elements of the entire ship energy system are built using a modular architecture. Notably, the significant improvements of ShipCLEAN-IWV focus on the ship's hydrodynamics in shallow and confined waterways. The aim is to present a physics-based model, which includes the interactions between the hull estimation, resistance predictions, propulsion, and engine, for a systematic approach to investigating the impact of dynamic inland waterways on energy consumption.

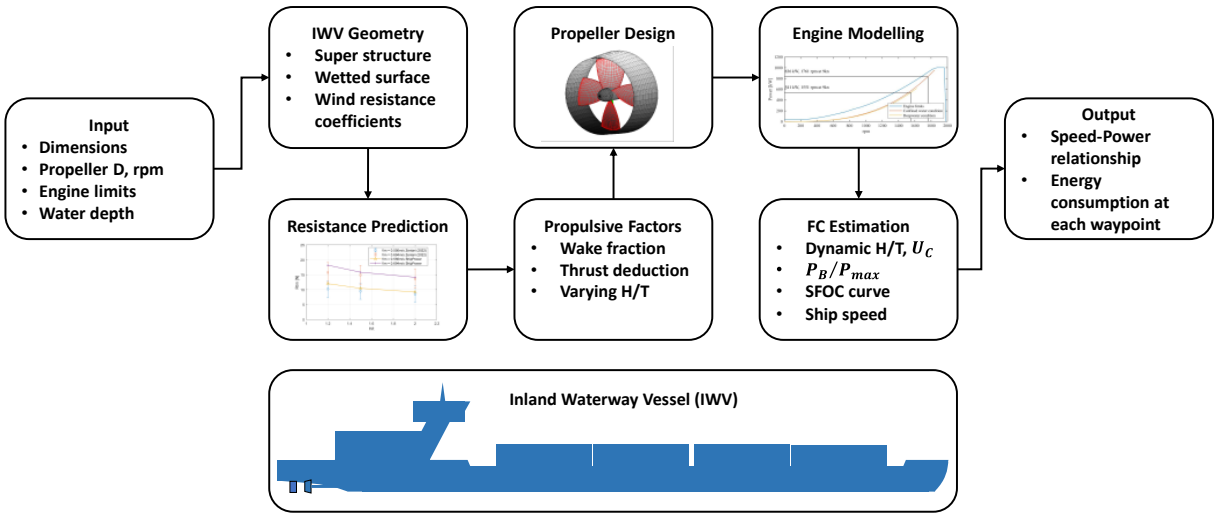

Figure 6. Overview of ShipCLEAN-IWV model (see Paper I).

2.1.1 Resistance in confined waterways

In the ShipCLEAN model, the equation for ship resistance prediction is given as follows:

$$R_T = 0.5\rho_{SW}{V_S}^2 S_W\left((1+k)C_F+C_R\right) + R_W + R_{AW} \quad (1)$$

where ρ_{SW} is the seawater density, V_s represents the ship's speed, S_W is the wetted surface area, k is the form factor, C_F is the frictional resistance coefficient, C_R is the residual resistance coefficient, R_W is the added wind resistance, and R_{AW} is the added wave resistance. Inland vessels constantly operate in relatively calm conditions without ocean waves and rarely suffer from strong wind or waves. Therefore, the new resistance module proposed here includes the factors specific to inland waterways, considering the influence of water depth and channel width (ship–bank distance). The total resistance in ShipCLEAN-IWV is calculated as:

$$R_T = 0.5\rho_{FW}{V_S}^2 S_W C_T + R_S + R_{BANK} \quad (2)$$

where ρ_{FW} is the freshwater density, R_S is the additional resistance due to squat in shallow water (Raven, 2016), R_{BANK} is the resistance induced from bank effect, and C_T is the total

resistance coefficient. The resistance estimation is based on the method from Zeng (2019), and the equation is given as follows:

$$C_T = \left(1+\left(k_{deep}+\Delta k\right)\right) C_F^* + C_W \tag{3}$$

where k_{deep} is the form factor from deep water and Δ_k is the additional form factor in shallow water. Instead of using the original method from Zeng (2019), a more generic method (Millward, 1989) was used since the former method for form factor correction is very sensitive to the ship's geometry. C_F^* is the frictional resistance coefficient, including the effect of water depth, and the equations to calculate Δ_k and C_F^* are given as:

$$\Delta\, k = 0.644 \left(\frac{H}{T}\right)^{-1.72} \tag{4}$$

$$C_F^* = \frac{0.08468}{(\log_{10} Re - 1.631)^2}\left(1 + \frac{c_1}{\log_{10} Re + c_2}\left(\frac{H}{T}\right)^{c_3}\right) \tag{5}$$

where H is water depth, T is the ship draught, c_1, c_2, and c_3 are parameters determined by ship type (see Table 1). In contrast to the conventional ITTC 57 correlation lines, in shallow water conditions, the frictional resistance depends not only on the Reynolds number Re, but also on the water depth-draught ratio. A similar result can be found in Zentari et al. (2022) as the C_F increases at lower UKC, especially when $H/T \leq 2.0$.

Table 1. Constants c_1, c_2, and c_3 for three baseline vessels (Zeng, 2019).

Vessel	C_B	c_1	c_2	c_3
Wigley hull	0.445	0.3466	–0.4909	–1.461
KCS	0.651	1.2050	–0.5406	–1.451
Rhine Ship 86	0.860	1.1680	–0.5238	–1.472

As suggested by Raven (2016), the additional squat effect in shallow water was also included to model the resistance increment. This method was built from towing tank tests and derived according to ship fullness and depth Froude number Fr_h. The equation is given as:

$$\Delta_{sinkage}/L = c_z \frac{\nabla}{L^3}\left[\frac{{Fr_h}^2}{\sqrt{1-{Fr_h}^2}} - \frac{{Fr_{hd}}^2}{\sqrt{1-{Fr_{hd}}^2}}\right] \tag{6}$$

where c_z is a parameter that depends on the hull shape and fullness, the average value is 1.46 (Raven, 2016), and $Fr_{hd} = \frac{V_S}{\sqrt{0.3gL}}$ is the depth Froude number in deep water conditions. The additional resistance from squat (R_S) can be computed from the equation:

$$R_S/R_T = \left(\Delta_{sinkage} A_{WP}/\nabla\right)^{2/3} \tag{7}$$

where A_{WP} is the ship's waterplane area, and ∇ is the ship's displacement (in m^3). The equation indicates that the additional resistance is calculated by the increment of the wetted surface area.

In addition to the influence of shallow water depth compared to the water depth at open sea, inland ships are also constrained by the channel width when sailing at a relatively short distance from the shore, especially on narrow fairways. A channel wall might induce additional hydrodynamic force on the ship's hull (Lataire et al., 2009; Vantorre, 2003; Zou & Larsson, 2013). The method for predicting such bank-induced resistance was formulated based on experimental data and simulation results (Du et al., 2020; Linde et al., 2017; Mucha et al., 2018); similarly, a noticeable resistance increment was observed when the ship–bank distance to beam ratio (d/B) decreased from approximately 2.5 to 1.0. Therefore, a regression curve was proposed according to the speed–depth relationship Fr_h and relative ship–bank distance d/B, as shown in Figure 7. It can be concluded from the collected data that the channel wall can induce up to 30% additional resistance if the ship sails close to the shore at high speed in confined waterways. By contrast, if such distance exceeds a specific range – that is, the ship is far from the shore – the bank effect can be neglected, and this range is calculated by an influential transversal distance y_{infl} (Lataire et al., 2009), given as:

$$y_{infl} = 5B(Fr_h+1) \tag{8}$$

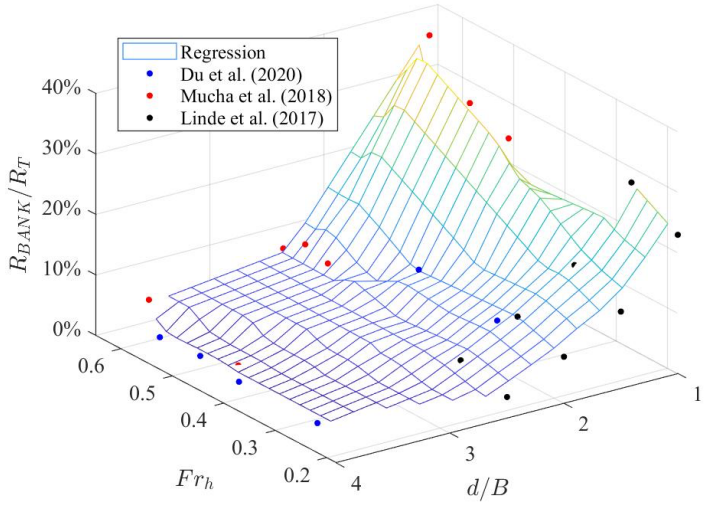

Figure 7. Regression curve for bank-induced resistance calculation, the surface was derived based on a collection of model test and simulation results.

2.1.2 Propulsion coefficients for IWVs

Apart from the resistance calculation, the propulsive factors (i.e., effective wake fraction w_E and resistance deduction t) also play a critical role in demanded power prediction. Accurately estimating these coefficients becomes challenging as most empirical methods have been developed only for sea-going vessels. The limited water depth influences the flow field around the propeller, resulting in strong disruptions and flow separations, which might significantly affect the wake and thrust deduction (Friedhoff et al., 2019; Kulczyk, 1995; Kulczyk & Tabaczek, 2014; Rotteveel et al., 2017). In addition, the prediction of t also depends on stern shapes and propeller configurations. The commonly used methods for sea-going vessels do not include the water depth effect, and their stern shapes and propulsion units significantly differ from inland vessels (often equipped with stern tunnels to increase the propulsion efficiency).

No empirical method is currently available for estimating these propulsive factors for inland vessels. Therefore, the research presented in this thesis utilised a relatively straightforward method by adapting the experimental value from the model test (Kulczyk & Tabaczek, 2014)

to generate a relatively accurate value, as the experiment was conducted specifically for European inland vessels with ducted propeller and stern tunnel, under various water depth and speed conditions (see Table 2). In terms of capturing dynamic depth conditions in inland waterways, the methods for the relatively deep-water case ($H/T \geq 3.0$) were also introduced, following the same empirical equations as used in the ShipCLEAN model.

Table 2. Method for predicting the wake w_E and t.

H/T	w_E	t
>=3.0	Kristensen and Lützen (2012)	Schneekluth and Bertram (1998)
2.7	0.22	0.20
2.0	0.27	0.24
1.8	0.23	0.27
1.6	0.20	0.27
1.4	0.26	0.29
1.2	0.32	0.30

The propeller was designed using the open-source tool OpenProp (Epps et al., 2009) in ShipCLEAN, where propellers can be designed and analysed based on a parametric standard series. However, the baseline blade geometries were primarily intended for standard commercial vessels. To capture the characteristics of real inland vessels, the propeller design module was modified with a focus on ducted propellers. The blade section details were acquired based on the classical Ka-470 type. Similarly, for the duct design, only a few airfoil types are available in OpenProp, so the duct design was extended by incorporating the NACA 4315 mean line, which has a very similar geometry to the classical N19A nozzle (see Figure 8).

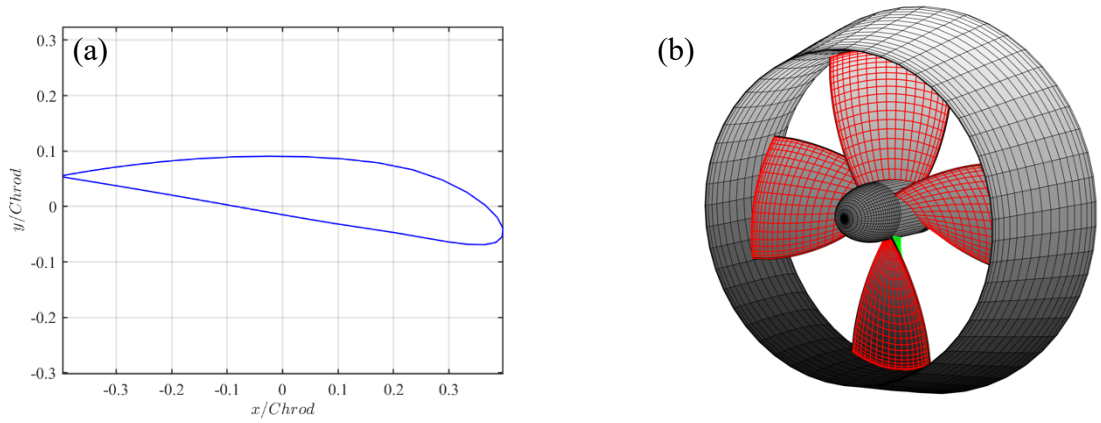

Figure 8. Ducted propeller design in ShipCLEAN-IWV.

In general, including the resistance result and propeller design, the demand shaft power (P_S) can be calculated using the following equation:

$$P_S = \frac{R_T V_S}{\eta_H \eta_O \eta_R \eta_S} \tag{9}$$

where η_H is the hull efficiency ($\eta_H = (1-t)/(1-w_E)$), η_O is the open water efficiency from the propeller curve, η_R is the relative rotative efficiency (where $\eta_R = 1.0$ as a constant), and η_S is the transmission efficiency including the shaft and gearbox loss, which is 0.97 in the present study.

2.1.3 Power and energy consumption analysis

The engine module in ShipCLEAN-IWV was derived based on a regression model using different engine curves from various suppliers and marine engine manufactures (Hidouche et al., 2015), such as Cummins, MAN, Caterpillar, and Wärtsilä, covering a wide range of operational power loads, as seen in Table 3. This model presents a straightforward method to estimate the specific fuel oil consumption ($SFOC$) dynamically based on the engine limit (P_{max}) and load ratio (P_S/P_{max}). During the early design stage, due to the limited available data for the target inland vessel, this model was regarded as an effective method for estimating energy consumption based on the existing ship design. By including more detail after this early stage, the engine model can be easily extended using a sophisticated module that includes variables such as fuel type and injection rate.

Table 3. Engine regression model based on load ratio (P_S/P_{max}).

P_{max} [kW]	$X = P_S/P_{max}$ [%]	$SFOC = f(X)$ [g/kW/h]	Error [%]
100–300	0–20	$398.89X^{-0.1987} + 8.945$	10
	20–100	$242.51 - 0.810X + 0.0065X^2$	7
300–500	0–20	$342.077X^{-0.1361}$	10
	20–100	$237.84 - 0.5957X + 0.0040X^2$	7
500–1000	0–20	$327.708X^{-0.1262} + 1.984$	15
	20–100	$230.192 - 0.4496X + 0.0033X^2$	10
1000–2000	0–20	$296.346X^{-0.0963} - 1.06$	10
	20–100	$236.786 - 0.7577X + 0.0064X^2$	10
2000–10000	0–20	$265.583X^{-0.0570} - 1.743$	7
	20–100	$240.204\ 0.9639X + 0.0064X^2$	5
>10000	0–20	$218.92X^{-0.0570} - 1.4368$	-
	20–100	$198 - 0.7945X + 0.0053X^2$	5

2.2 Manoeuvring model development

In terms of manoeuvring tests to predict ship motions, the methods used in existing research can be divided into free-running methods, which directly conduct tests with an acting propeller and rudder, and system/mathematical model-based methods, which involve solving rigid body dynamic equations. Due to the high cost and numerical complexity of physical and numerical free-running tests, most studies focus on the latter method by calculating hydrodynamic force to formulate rigid-body ship equations (manoeuvring models) for predicting the ship's trajectory. The most important task here is to accurately compute the hydrodynamic force under different speeds and drifting angles, the so-called hydrodynamic derivatives. This subchapter first introduces commonly used manoeuvring models on open water and their limitations, then develops a new manoeuvring model specifically for inland vessels that includes the shallow water and bank effect.

2.2.1 Manoeuvring model in open water

The past decades have seen active research on ship manoeuvring tests and mathematical models. These manoeuvring models can be divided into three types: (i) the response model, (ii) the whole ship model, and (iii) the modular model. Nomoto et al. (1957) proposed the response model, also known as the KT model, in which the ship's motion is represented by a turning

ability index (K) and a course-keeping index (T). This simplified model aims to generate a fast ship trajectory prediction and has thus been widely used in control studies of marine surface vessels (Fossen, 2011). However, one considerable shortcoming of the KT model is that even after introducing a damping term (Norrbin, 1977), the hydrodynamic effect is still over-simplified.

In contrast, a whole ship model (Abkowitz, 1964) was proposed to include the impact of ship hydrodynamics and environmental disturbances, such as wind, waves, and ocean currents, where the force and moment acting on the ship's hull are represented by a Taylor series. Ogawa and Kasai (1978) proposed another ship mathematical model, the manoeuvring modelling group (MMG) model, which decomposes the force and moment groups by analysing the impacts of individual elements, such as the hull, propeller, and rudder. Comparing the features of these two ship mathematical models, the whole ship model is suitable for analysing the overall ship's manoeuvring performance for free running tests and system identification studies, while the modular MMG model can be used to better understand the influence of individual components (Clarke, 2003; Liu et al., 2015).

The modular architecture of the MMG model gives it a significant advantage. Though it was initially developed for conventional sea-going vessels and may not be directly applicable to inland water conditions, it can be modified by incorporating additional factors, such as the shallow water and bank effects. Therefore, a modified MMG model was developed specifically for IWVs, and the detailed equations are presented in this subsection.

2.2.2 Manoeuvring model for IWVs

Inland vessels constantly operate in a relatively calm environment compared to ocean-going vessels. Therefore, a two-dimensional (2D) planar ship motion with three degrees of freedom (3-DoF) is suitable for estimating the ship's motions (surge, sway, and yaw), as inland vessels do not experience strong vertical motions, such as heave and pitch from ocean waves. The coordinate systems are indicated in Figure 9; the vessel moves in an earth-fixed coordinate system, denoted by $o_0 - x_0 y_0 z_0$, where the midship is selected as the origin of the body-fixed system $o - xyz$.

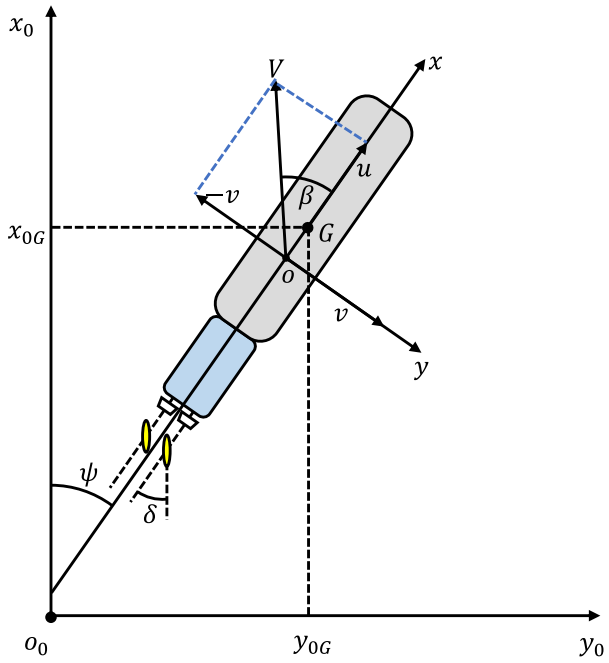

Figure 9. Coordinate systems used for inland vessels.

The centre of gravity (CoG) is G with coordinates $(x_G, 0,0)$ in the ship-fixed system, and the rudder angle and heading are represented by δ and ψ, respectively. This study focuses primarily on inland vessels with twin-propeller twin-rudder (TPTR) configuration.

2.2.3 Equations of motion

The manoeuvring model for motion prediction on inland waterways was derived based on the original MMG method, with modifications for the shallow water and bank effects. The manoeuvring equations are given as follows:

$$\left.\begin{aligned}(m+m_x)\dot{u} - \left(m + m_y\right)v_m r - x_G m r^2 &= X_H + X_P + X_R + X_B \\ (m+m_x)\dot{v}_m - (m+m_x)ur + x_G m\dot{r} &= Y_H + Y_R + Y_B \\ (I_z+x_G^2 m+J_Z)\dot{r} + x_G m(\dot{v}_m+ur) &= N_H + N_R + N_B\end{aligned}\right\} \quad (10)$$

The left-hand side follows the original MMG model, where m is the ship's mass, m_x and m_y denote the added mass in the x and y-directions, respectively, x_G is the longitudinal coordinate of CoG, I_z represents the moment of inertia, and J_z is the added moment of inertia for yaw motion. On the right-hand side, the X, Y, N represent the surge force, sway force, and yaw moment, respectively. The subscripts H, P, R represent the individual force and moment from the ship's hull, propeller, and rudder, respectively, as the original MMG indicates. The shallow water effect was included in the hull part, and another new item with subscript B to calculate the bank effect was introduced. The overall model architecture was built in the MATLAB environment. Figure 10 shows the model setup and architecture, and the formulation of individual blocks is described in subsequent sections.

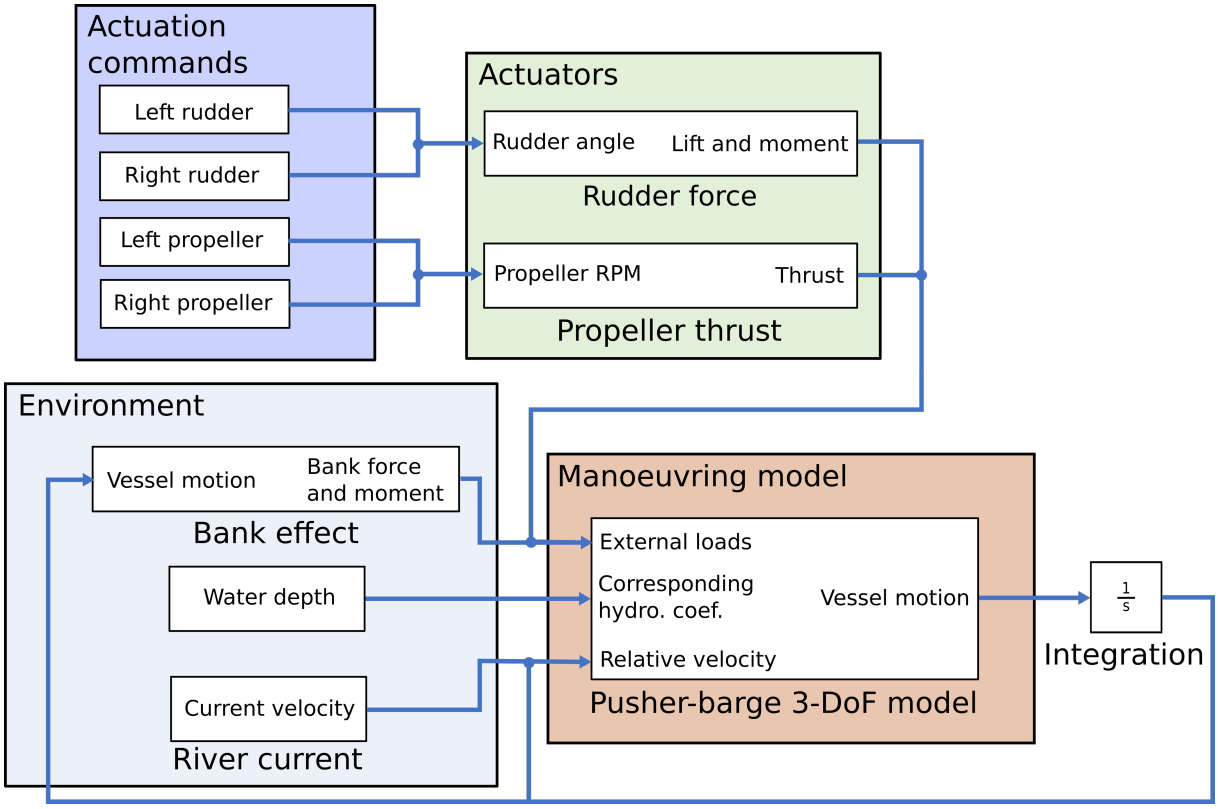

Figure 10. A schematic of the manoeuvring model architecture presented in Paper II.

2.2.4 Hydrodynamic forces on the ship hull

The equations of hydrodynamic force and moment acting on the ship's hull are given below:

$$\left.\begin{aligned} X_H &= 0.5\rho LTU^2 X'_H \\ Y_H &= 0.5\rho LTU^2 Y'_H \\ N_H &= 0.5\rho L^2 TU^2 N'_H \end{aligned}\right\} \tag{11}$$

where ρ represents the freshwater density, L is the ship's length, T is the draught, U is the ship's speed, X'_H, Y'_H, N'_H represent the non-dimensional surge force, sway force, and yaw moment, respectively, calculated from equations:

$$\left.\begin{aligned} X'_H &= -R'_0\, cos^2\,\beta_m + X'_{\beta\beta}\beta_m^2 + X'_{\beta r}\beta_m r' + X'_{rr}r'^2 + X'_{\beta\beta\beta\beta}\beta_m^4 \\ Y'_H &= Y'_\beta\beta_m + Y'_r r' + Y'_{\beta\beta\beta}\beta_m^3 + Y'_{\beta\beta r}\beta_m^2 r' + Y'_{\beta rr}\beta_m r'^2 + Y'_{rrr}r'^3 \\ N'_H &= N'_\beta\beta_m + N'_r r' + N'_{\beta\beta\beta}\beta_m^3 + N'_{\beta\beta r}\beta_m^2 r' + N'_{\beta rr}\beta_m r'^2 + N'_{rrr}r'^3 \end{aligned}\right\} \tag{12}$$

Here, R'_0 is the non-dimensional total resistance coefficient, including a correction for water depths, $X'_{\beta\beta}$, $X'_{\beta r}$, …, N'_{rrr} are the so-called hydrodynamic derivatives, β_m is the mid-ship drift angle, computed as $\beta_m = -\tan^{-1}(v_m/u)$, and r' is the non-dimensional yaw rate ($r' = rL/U$).

2.2.5 Propeller model

The equation for a twin-propeller configuration is given as:

$$X_P = (1-t)(T_P^P + T_P^S) \tag{13}$$

where t is the thrust deduction factor, T_P^P and T_P^S are the propeller thrust forces from the portside and starboard, respectively, given as:

$$T_P^P = T_P^S = \rho n_P^2 D_P^4 K_T \tag{14}$$

where n_P is the propeller speed, D_P is the propeller diameter and K_T is the thrust coefficient:

$$K_T = k_2 J^2 + k_1 J + k_0 \tag{15}$$

where k_1 and k_2 are regression parameters from open water curves, and J is the advance ratio:

$$J = u(1-w_P)/(n_P D_P) \tag{16}$$

In Eq. (16), u is the ship surge velocity, and w_P is the wake fraction during ship steering, which is calculated as the following equation:

$$w_P/w_{P0} = \exp(-4\beta_P^2) \tag{17}$$

where w_{P0} is the wake fraction for straight motion and β_P is the propeller inflow angle during manoeuvring ($\beta_P = \beta - (x_P/L)\,r'$), depending on the relative coordinate of the propeller x_P. Notably, the parameters of the propeller on each side, such as t and w_{P0}, are assumed to be identical for model simplification. This is because an accurate analysis of unsymmetrical inflow for twin propellers during steering is complicated, requiring the experimental measurement of the flow field or detailed CFD simulations, which is out of the scope of the model development.

2.2.6 Rudder model

The rudder force and moment are essential to vessels' steering performance. The corresponding equations are given as:

$$\left.\begin{aligned} X_R &= -(1-t_R)(F_N^P+F_N^S)\sin\delta \\ Y_R &= -(1+\alpha_H)(F_N^P+F_N^S)\cos\delta \\ N_R &= -(x_R+\alpha_H x_H)(F_N^P+F_N^S)\cos\delta \end{aligned}\right\} \tag{18}$$

where t_R is the steering resistance deduction factor, F_N is the rudder normal force, α_H represents the rudder force increase factor, x_R is the relative longitudinal coordinate of the rudders and is identical on each side, and x_H is the longitudinal coordinate of the location at which the additional lateral force is acting. F_N is computed as:

$$F_N = 0.5\rho A_R U_R^2 C_N \tag{19}$$

where A_R is the rudder area, U_R is the flow velocity at the rudder ($U_R = \sqrt{u_R^2 + v_R^2}$), and C_N is the rudder normal force coefficient based on the original MMG model, given as:

$$C_N = \frac{6.13\Lambda}{\Lambda + 2.25}\sin\alpha_R \tag{20}$$

where Λ is the rudder aspect ratio ($\Lambda = B_R/C_R$, where B_R is the rudder span and C_R is the chord length), and α_R is the effective rudder inflow angle, calculated using the equation:

$$\alpha_R = \delta - \tan^{-1}\left(\frac{v_R}{u_R}\right) \tag{21}$$

where u_R is the longitudinal rudder inflow speed, and v_R is the transverse rudder inflow speed, calculated using the following equation:

$$\begin{aligned} v_R &= U\gamma_R(\beta - l_R' r') \\ u_R &= \frac{\varepsilon u_P}{1-s}\sqrt{1 - 2(1-\eta\kappa)s + \{1-\eta\kappa(2-\kappa)\}s^2} \end{aligned} \tag{22}$$

where γ_R represents the flow straightening coefficient, l_R' is a constant of the acting point of v_R collected from the model test, and ε is the ratio of wake fraction of the rudder to the propeller $\varepsilon = (1 - w_R)/(1 - w_P)$. Based on Koh and Yasukawa (2012), in the equation for calculating u_R, s stands for the propeller slip ratio, η is a relative ratio of propeller diameter to rudder span, as $\eta = D_P/B_R$, and κ is an experimental constant.

2.2.7 Mathematical model of bank effect

When a ship is sailing close to the bank, especially on confined waterways, the accelerated flow in the gap between the ship and the bank results in a pressure difference between the sides, particularly around the acting propeller. This induces an additional lateral force and yaw moment to the ship, affecting the ship's heading (see Figure 11).

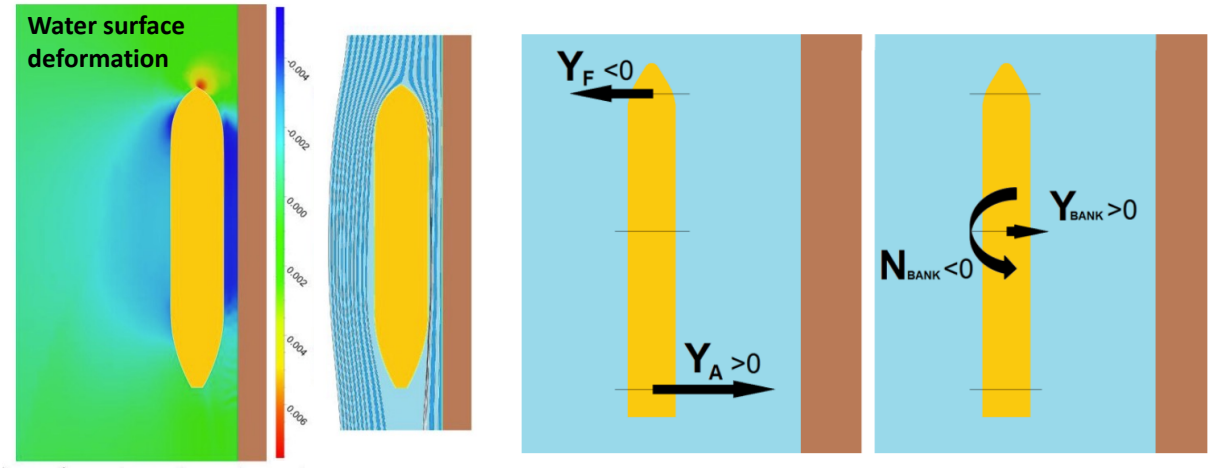

Figure 11. Bank effect schemes, reproduced from Lataire et al. (2018).

The mathematical model proposed by Vantorre et al. (2003) was used to calculate the bank effect. This model was derived from an experimental study based on the force and moment measured under various speed and ship–bank distance conditions:

$$\left.\begin{aligned} Y_B^H &= 0.5\rho LTu^2 \sum_{i=1}^{2}\sum_{k=0}^{2} a_{ik}^H y_B^i \left(\frac{T}{H-T}\right)^k \\ N_B^H &= 0.5\rho L^2 Tu^2 \sum_{i=1}^{2}\sum_{k=0}^{2} \beta_{ik}^H y_B^i \left(\frac{T}{H-T}\right)^k \\ Y_B^P &= 0.5\rho LTV_T^2 \sum_{i=1}^{2}\sum_{k=0}^{2} a_{ik}^P y_B^i \left(\frac{T}{H-T}\right)^k \\ N_B^P &= 0.5\rho L^2 TV_T^2 \sum_{i=1}^{2}\sum_{k=0}^{2} \beta_{ik}^P y_B^i \left(\frac{T}{H-T}\right)^k \\ Y_B^{HP} &= 0.5\rho LTV_T^2 Fr \sum_{i=1}^{2}\sum_{k=0}^{2} a_{ik}^{HP} y_B^i \left(\frac{T}{H-T}\right)^k \\ N_B^{HP} &= 0.5\rho L^2 TV_T^2 Fr \sum_{i=1}^{2}\sum_{k=0}^{2} \beta_{ik}^{HP} y_B^i \left(\frac{T}{H-T}\right)^k \end{aligned}\right\} \quad (23)$$

The superscripts H, P, HP denote the individual effects of pure speed (hull), propulsion, and coupled effect; V_T is the reference velocity; Fr is the Froude number; and α_{ik}^H, β_{ik}^H, α_{ik}^P, β_{ik}^P, α_{ik}^{HP}, and β_{ik}^{HP} are coefficients from regression analysis. Detailed parameters can be found in Vantorre et al. (2003).

2.3 Control system design

In terms of ships operating on confined waterways, especially when a vessel sails close to one side of the channel to give way to another vessel passing head-on or overtaking the first vessel, effective rudder actions are needed to counteract the hydrodynamic effects from the banks to ensure safety (Eloot & Vantorre, 2011). The rudder should generate enough steering moment to stabilise the ship's heading under the bow out moment (see Figure 12).

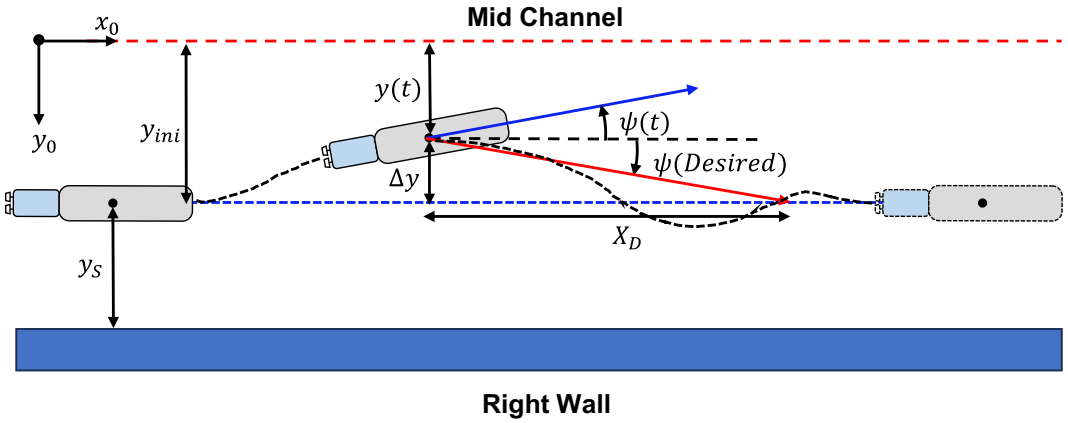

Figure 12. Illustration of heading control under bank effect.

Therefore, a proportional-derivative (PD) controller was developed to adjust the rudder angle and incorporated into the manoeuvring simulation, represented by:

$$\delta_C = -K_P\left(\left(\psi - \psi_{Ref}\right) + T_D\frac{d\left(\psi - \psi_{Ref}\right)}{dt}\right) \tag{24}$$

where δ_C is the command rudder angle, K_P is the controller P-gain, T_D is the controller derivative time, ψ is the current ship heading, and ψ_{Ref} is the desired heading angle, defined by:

$$\psi_{Ref} = \begin{cases} 0 & \text{(Mid-channel)} \\ \tan^{-1}\left(\dfrac{\Delta y}{X_D}\right) & \text{(Sailing along banks)} \end{cases} \tag{25}$$

Eq. (25) shows two typical operational conditions on confined waterways when the desired course is mid-channel. For example, to mitigate the unsymmetrical hydrodynamic effect on highly narrow waterways, the ship will take a zero heading as a reference. The other operational condition involves sailing close to one bank at a relatively constant lateral distance to clear the way for other vessels, where the ship might suffer from a strong bank effect at a shorter ship–bank distance. Therefore, in Eq. (25), Δy is the difference between the current lateral position ($y(t)$) and the desired lateral position (y_{ini}), which is defined as $\Delta y = y_{ini} - y(t)$, and X_D is a predefined length to represent the triangle in Figure 12 (80 m used in this study).

River currents are another factor which affects the inland vessel's manoeuvring performance. The rudder control also includes the current effect by utilising a reference ship velocity, and according to Fossen (2011), the relative velocity is given as:

$$\begin{aligned} u_r &= u - U_C\cos(\beta_C - \psi) \\ v_r &= v - U_C\sin(\beta_C - \psi) \end{aligned} \tag{26}$$

where β_C is the angle of the incoming current, which is 180° when the ship is sailing upstream and 0° for downstream sailing.

3 Results

This chapter summarises the results presented in the appended Papers I and II. The following sections highlight the most important results and findings.

3.1 Summary of Paper I

Paper I describes the development of a holistic ship energy performance model, ShipCLEAN-IWV, designed for general application to inland vessels. The model retains the modular architecture of ShipCLEAN, initially developed for sea-going vessels, while incorporating new methods to model the hydrodynamic effects of confined waterways and to capture the specific characteristics of inland ships. The resistance prediction was modified using a combination of empirical equations for shallow water, with the results demonstrating very good accuracy in a verification study based on available experimental measurements. Power prediction was also validated through the publicly available literature. Additionally, an operational case study was conducted using data from stretches of waterways under dynamic water depth and width conditions to investigate the impact of loading and ship–bank distances on global ship energy consumption.

3.1.1 Verification study

As discussed in Section 2.1, the most important factor for power prediction is the accuracy of the resistance prediction. The new resistance calculation involves a combination of modified calm water resistance (primarily on the viscous part), additional squat, and bank-induced drag. The verification study using experimental data from a scaled self-propelled vessel (Mucha et al., 2018) is shown in Figure 13. The results show that the proposed model's results generally agree very well with the model test data. The model can capture the change in resistance at varying water depths. Despite the differences observed at high ship speeds in extremely shallow water (H/T = 1.2), this discrepancy may be attributed to the neglect of correction for wave-making resistance. Inland vessels typically reduce speed in low water level conditions due to potential grounding risks due to squat.

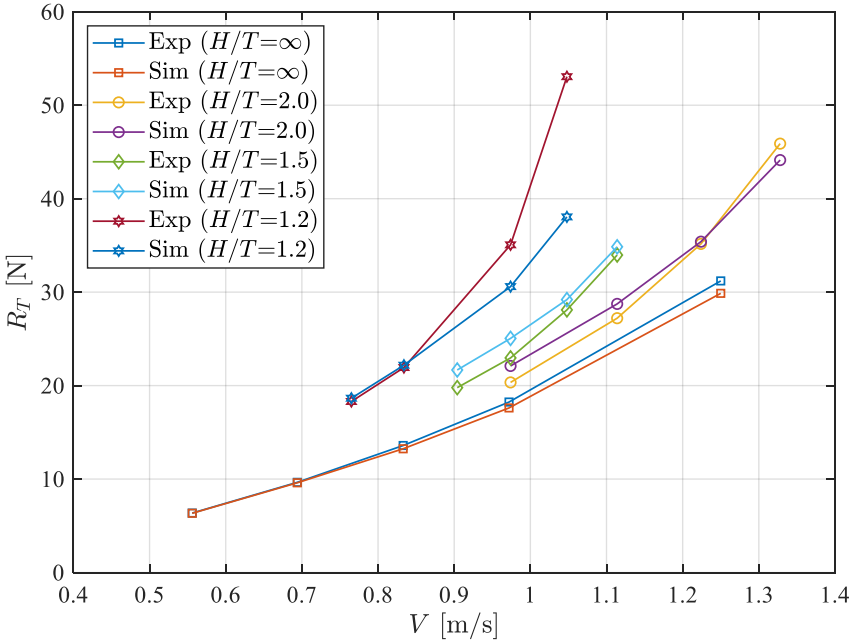

Figure 13. Resistance prediction for self-propelled inland vessels.

In addition to self-propelled vessels, another commonly used type of inland vessel, the pusher–barge system, was also investigated by collecting towing tank test data from pusher–barge convoys under various barge configurations (Zentari et al., 2022), as shown in Figure 14. The comparison summary in Figure 15 shows that the ShipCLEAN-IWV predictions fall within the scatter of the experimental measurements. The summary reveals a similar trend in which the resistance difference increases with decreasing water depth. In addition to the previously mentioned issue of neglected wave-making resistance, stronger interactions and gap flows between the barges also contribute to the resistance; the gap between a single barge and pusher can induce up to 6% of the total resistance (Zentari et al., 2023). However, these factors depend strongly on vessel shape and speed, which are beyond the scope of this study.

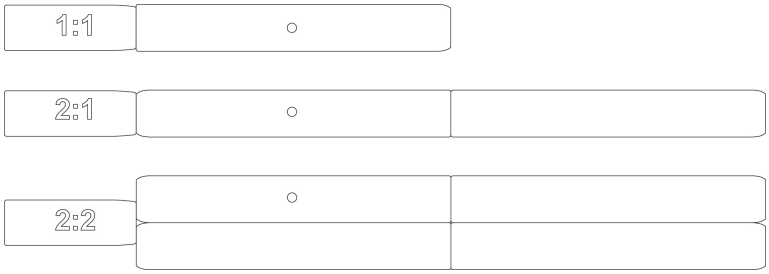

Figure 14. Pusher barge configurations in the model test (Zentari et al., 2022).

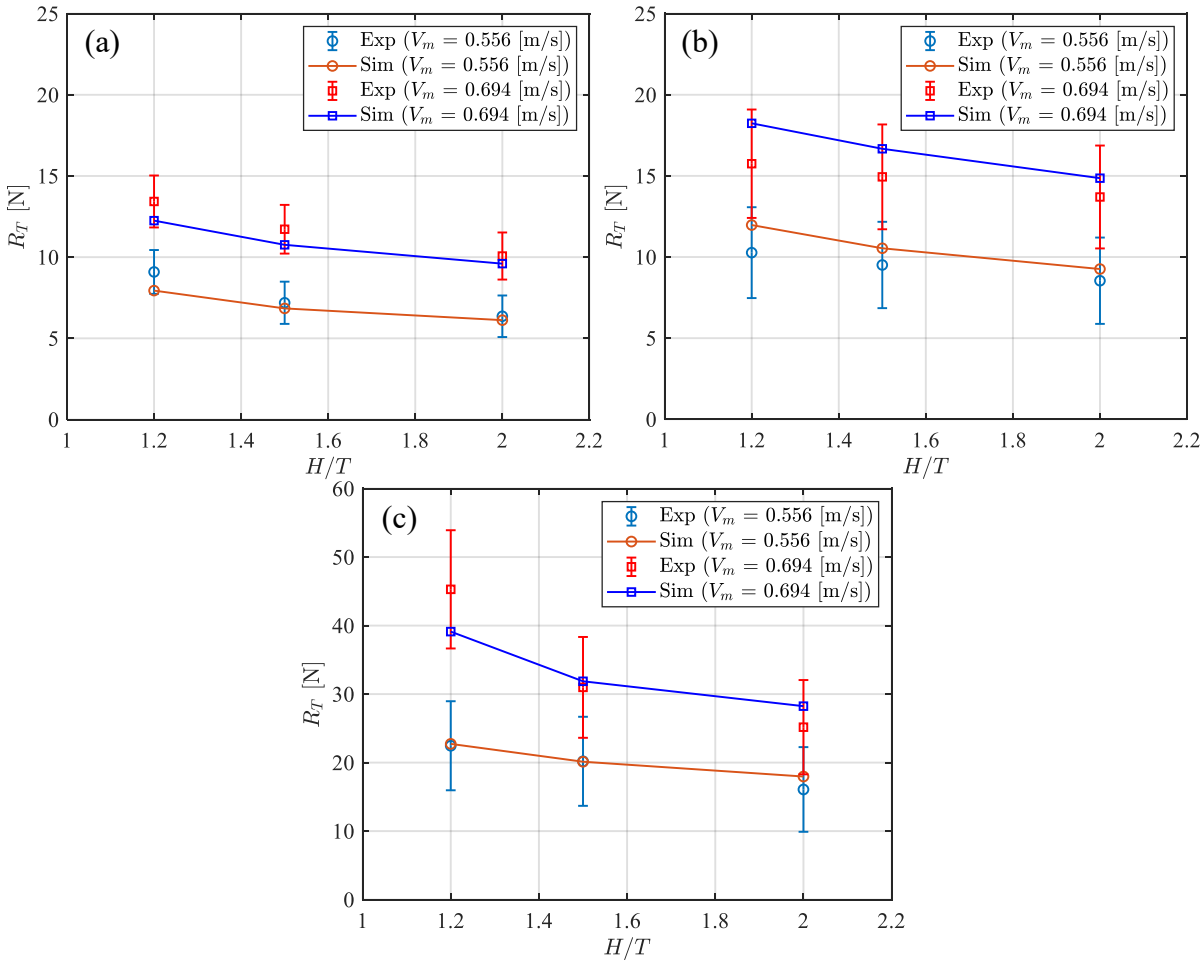

Figure 15. Resistance prediction for pusher–barge convoys:
(a) 1:1 configuration, (b) 2:1 configuration, and (c) 2:2 configuration.

3.1.2 Operational analysis

A typical self-propelled inland vessel was utilised for the dynamic operational analysis. The ship has a length of 135 m, a beam of 11.45 m, and a design draft of 3.2 m under a 90% loading condition; see other loading conditions in Table 4. The water depths (H) were selected from a 153 km length of the Seine River (Linde, 2017), and the corresponding width data (W_C) was acquired from the MERIT Hydro database (Yamazaki et al., 2019). Using the recorded discharge rate, the current speed (U_C) along the waypoints was calculated (see Figure 16).

Table 4. Vessel displacement under various loading conditions.

Loading rate [-]	Displacement [t]	T [m]	S_W [m^2]
40%	2590	1.85	1859.01
60%	3390	2.40	2014.94
80%	4190	2.94	2169.12
100%	4990	3.50	2323.83

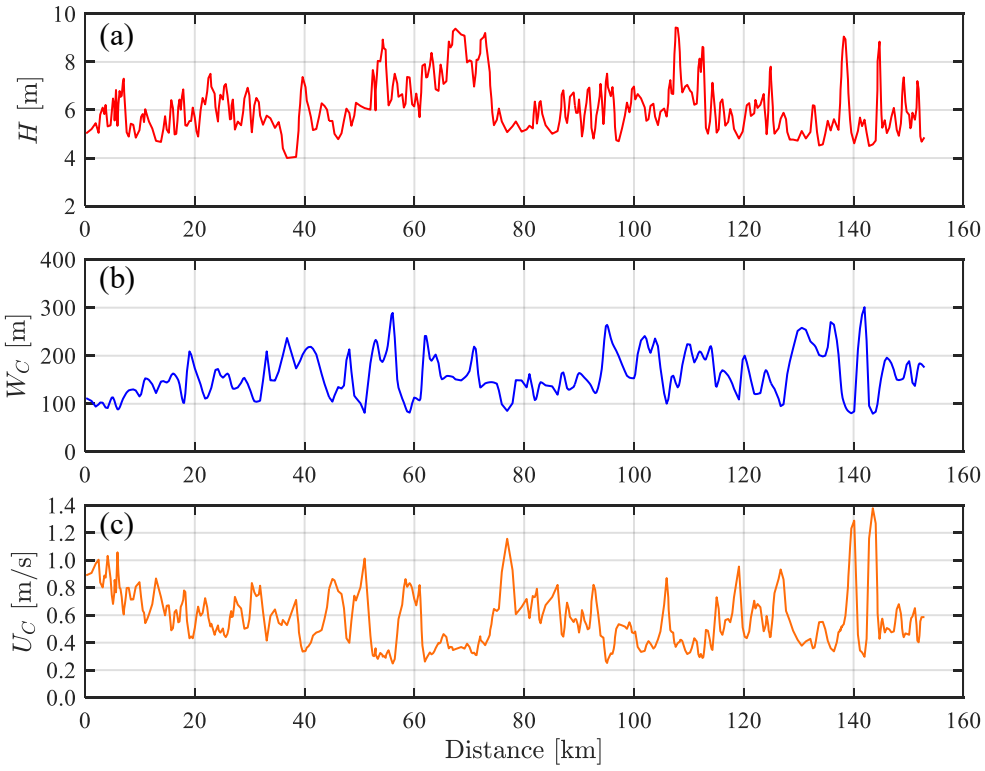

Figure 16. Waterway data of the selected reach with a length of 153 km.

The power result and corresponding instant fuel consumption are shown in Figure 17. Notably, under shallow water conditions, the increase in loading (draught) has a significant impact on power demand and fuel consumption. The shallowest water results in a 70% power increase and additional fuel consumption at 40% loading and up to a 100% increase under fully loaded conditions.

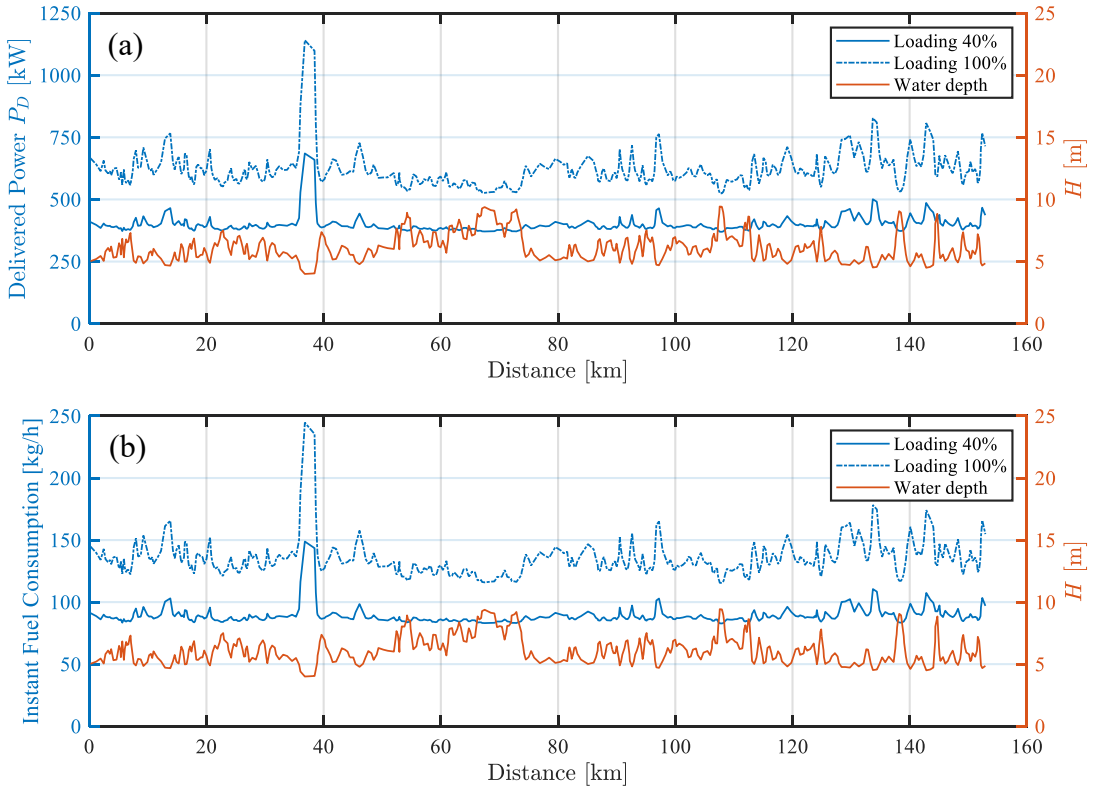

Figure 17. Power (a) and fuel consumption (b) rate under various loading conditions.

In addition to water depth, the effect of the ship–bank distance on fuel consumption was also investigated, as shown in Figure 18. Distances d_1 and d_2 represent ship–bank distances of one-half and one-quarter of the channel width, respectively. As the blue bounding box indicates, a noticeable change in resistance occurs when the ship sails at a relatively short distance from the shore. However, bank effects generally have a minor impact on resistance compared to the shallow water effect.

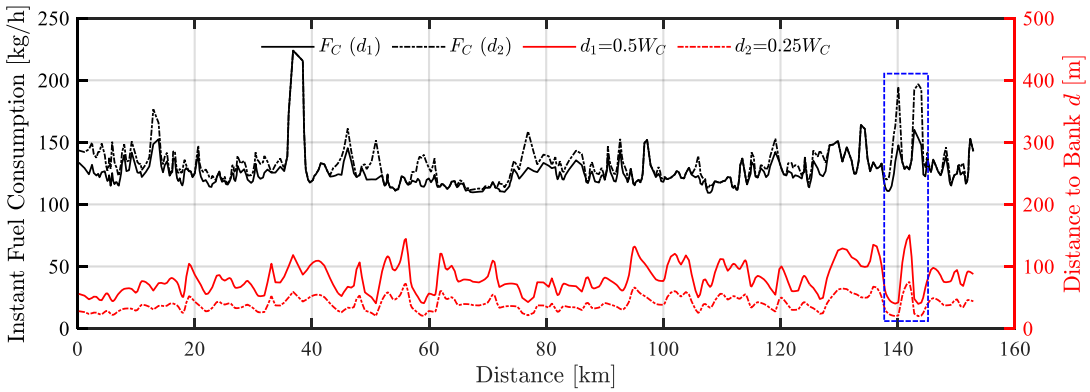

Figure 18. Fuel consumption rate under dynamic ship–bank distances.

3.2 Summary of Paper II

Paper II presents a manoeuvring model specifically designed for IWVs. Based on the 3-DoF MMG method, the model incorporates a shallow water correction and a mathematical representation for bank effects to predict the vessel's manoeuvring behaviour, particularly in confined waterways. The simulation began with a verification study, in which the turning simulation was performed using hydrodynamic derivatives from the literature. Subsequently, the effect of the

bank on the vessel's trajectory was individually analysed (without rudder execution) under various water levels, ship–bank distances, and propeller speeds. Additionally, a case study was conducted to test the performance of the rudder controller in counteracting bank-induced hydrodynamic force to stabilise the predetermined course.

3.2.1 Verification simulation

The verification was performed based on experimental data from a pusher–barge model in calm water, which did not initially include the bank effect. The aim was to evaluate the model's accuracy using hydrodynamic derivatives from the publicly available literature. The turning simulation was conducted at two rudder angles, δ = 35° and δ = 20°, at a speed of U = 0.364 m/s (5 knots at full-scale). Notably, the original paper (Koh & Yasukawa, 2012) neglected the fourth-order derivative $X'_{\beta\beta\beta\beta}$; see Eq. (12). Selected results for the turning comparison are presented in Figure 19 and Figure 20, where 'simulation' refers to the developed manoeuvring model. Generally, the manoeuvring model can capture the vessel's manoeuvring performance. The pusher barge demonstrates even better turning ability in shallow water. This is attributed to the shape of the pusher, which is similar to that of wide-beam ships.

Deviations in the turning circle, such as those seen in Figure 20(b), might be caused by the underestimation of the rudders' normal force coefficient by the empirical formula. This may also be due to missing parameters in the literature. Consequently, the coordinates of the centre of gravity (CoG) and the relative positions of the propeller and rudder must be estimated. The deviation of these acting points from the original ship model can affect the value of the rudder normal force.

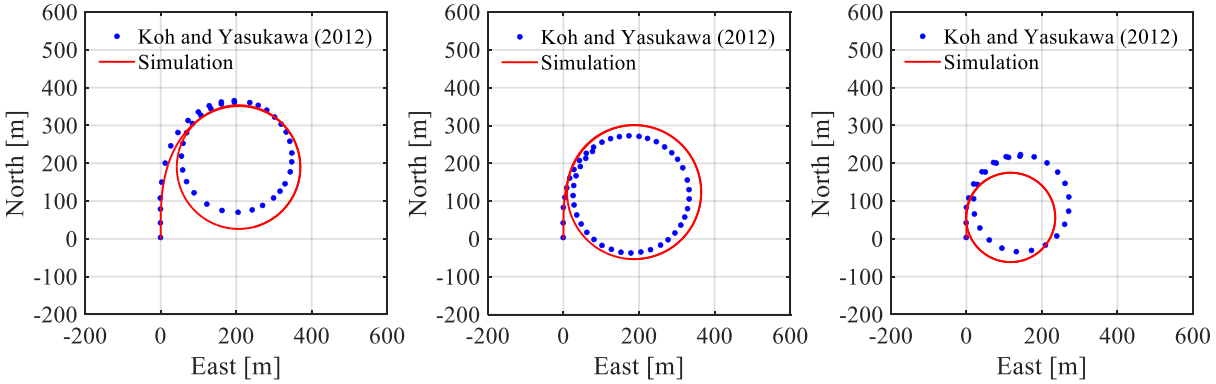

(a) H/T = 19.3 (b) H/T = 1.5 (c) H/T = 1.2

Figure 19. Model verification on turning at δ = 35°.

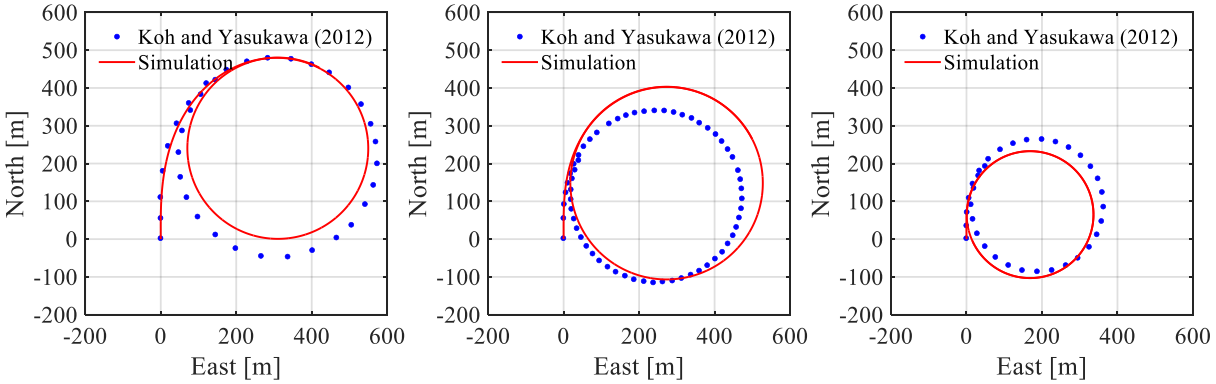

(a) H/T = 19.3 (b) H/T = 1.5 (c) H/T = 1.2

Figure 20. Model verification on turning at δ = 20°.

The results for the tactical diameters at each water depth are summarised in Figure 21. The overall comparison indicates good accuracy of the manoeuvring model, as the tactical diameter agrees well with the full-scale data from the manoeuvring study in the literature.

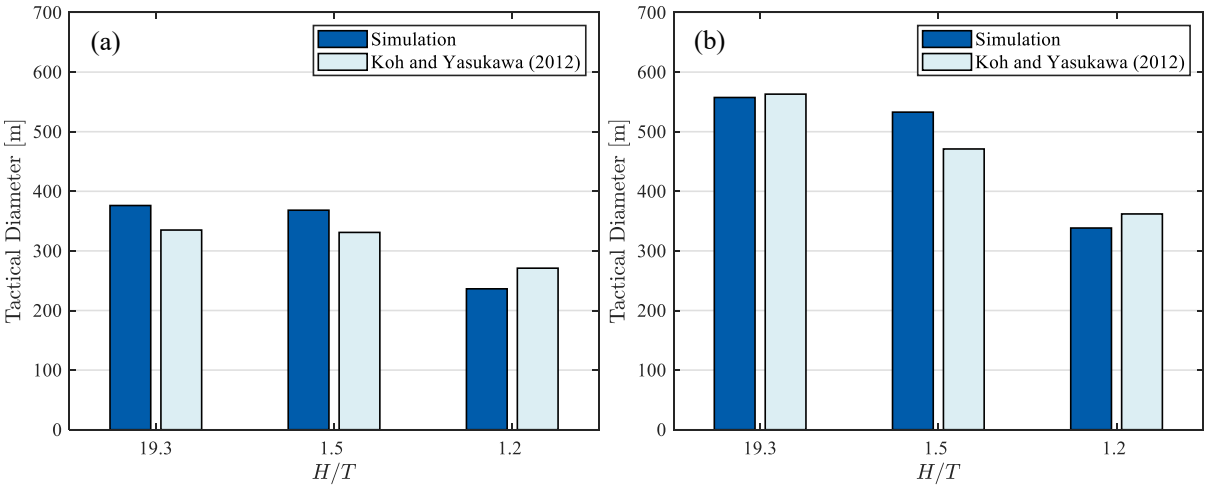

Figure 21. Comparison of tactical diameters at each rudder angle: (a) $\delta = 35°$ and (b) $\delta = 20°$.

3.2.2 Sensitivity analysis on hydrodynamic derivatives

Hydrodynamic derivatives are crucial to manoeuvring simulation models. A sensitivity analysis was performed to find the dominate terms (see Figure 22). The linear terms were found to be the most important regarding the sensitivity value. In addition, nonlinear terms, such as $N_{\beta\beta\beta}$, $N_{\beta\beta r}$, and $N_{\beta rr}$, become noticeable when the vessel carries out tight manoeuvres, that is, when the rudder angle increases from 20° to 35°, as shown in Figure 22(b). This insight is vital for manoeuvring studies since contemporary European inland vessels typically have flexible rudders (the rudder angle can be up to 90°). Regression analysis on these non-linear hydrodynamic terms should be carefully examined.

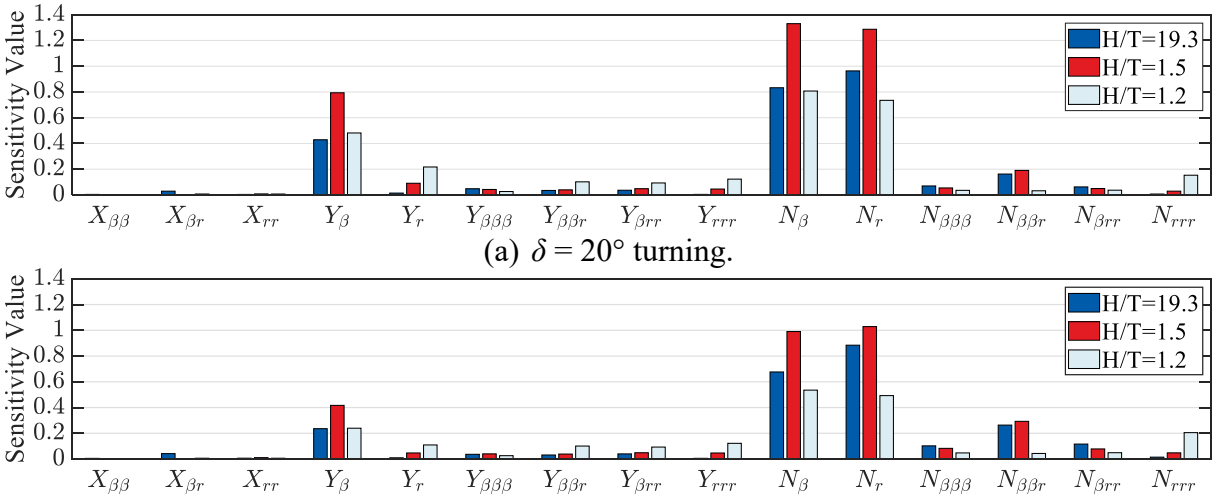

(a) $\delta = 20°$ turning.

(b) $\delta = 35°$ turning.

Figure 22. Sensitivity analysis on the hydrodynamic derivatives.

3.2.3 Bank effect simulations

Simulations on bank effects were conducted to investigate the vessel's motion solely under bank hydrodynamic effects (without rudder control). The ship was assumed to sail in a straight channel with a width of 100 m at various initial starboard–bank distances y_S, as seen in Figure 23. The simulation time was set to 140 seconds for all the cases. The trajectories indicate that

the ship is subject to a minor bank effect when travelling close to the waterway centre. However, as y_S decreases, the bow-out movement due to the unsymmetrical flow between the portside and starboard becomes significant. The ship experiences a noticeable course deviation and even shows a risk of colliding with the opposite bank.

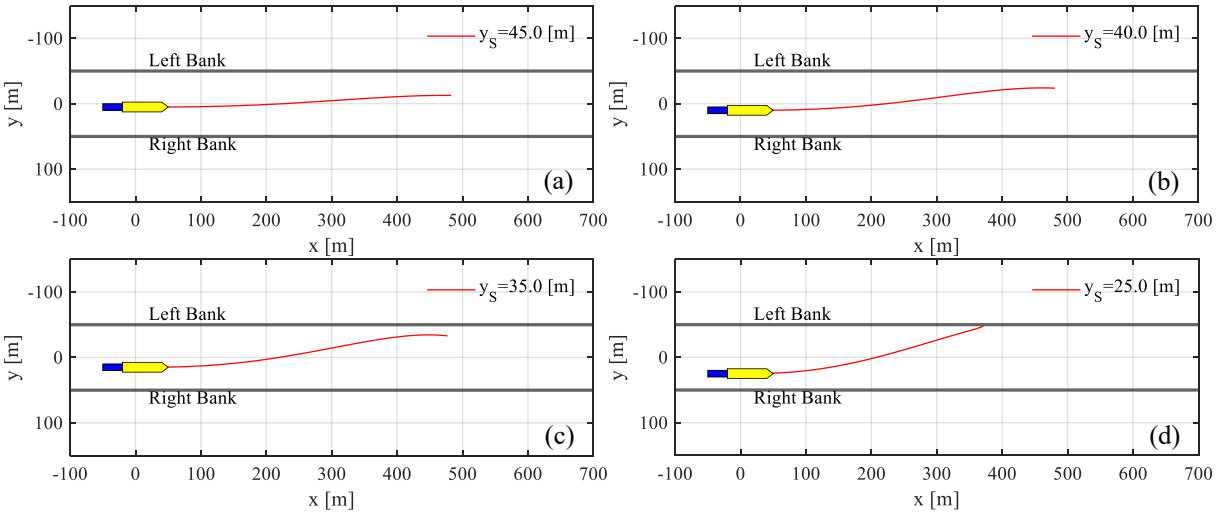

Figure 23. Vessel trajectory under bank effect with different y_S (H/T = 19.3) at an initial vessel speed of 5 knots and propeller revolution speed of 150 rpm.

Simulations of bank effects at various water depths are presented in Figure 24. Compared to deep water, the bank effects on the vessel's motion become more evident in shallow water, as the decreased water depth makes the unsymmetric phenomenon more significant.

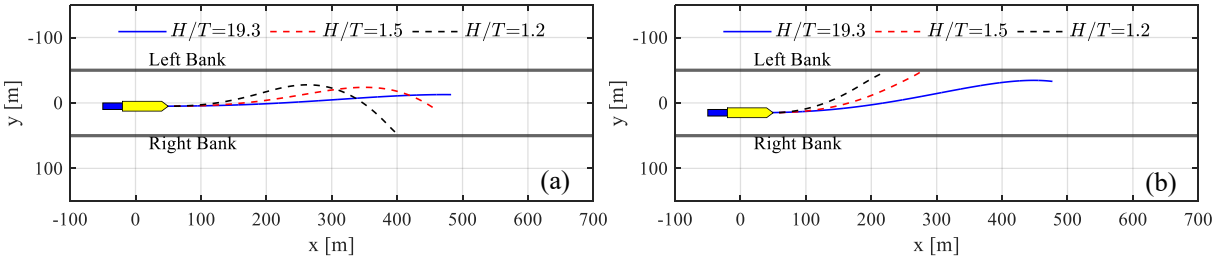

Figure 24. Ship trajectories at three different water depths: (a) y_S = 45 m and (b) y_S = 35 m.

In addition, the impact of the acting propeller was analysed and quantified. The simulation indicates that an increased propeller speed can aggravate the effect on the hull, thereby increasing the risk of collision with the shore, as seen in Figure 25. Eq. (23) indicates that the individual hydrodynamic effect increases at a higher propeller revolution speed. This contributes to the bank-induced force and moment, resulting in ship manoeuvring difficulties.

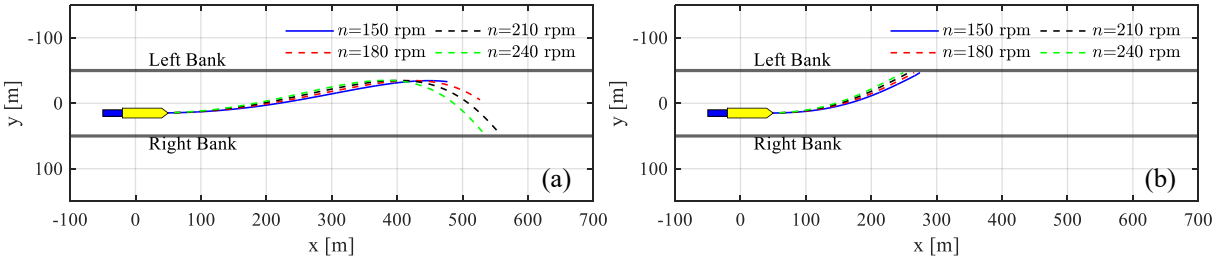

Figure 25. Bank effects at various propeller speeds (y_S = 35 m): (a) H/T = 19.3 and (b) H/T = 1.5.

3.2.4 Rudder control simulation

To ensure the vessel's navigation safety on inland waterways, the rudder capacity must be carefully checked to ensure it delivers enough steering force and moment. Especially when a vessel is passing through a highly confined channel, effective rudder control is necessary to counteract the bank effects and stabilise its target course. Therefore, rudder control simulations were conducted under two typical operational scenarios: (a) adjusting the heading to sail mid-channel and (b) sailing along one bank to clear the channel for oncoming or passing vessels. Figure 26 shows the vessel trajectory for mid-channel navigation under river currents in different directions. Based on the time histories of rudder execution (Figure 27), it can be concluded that the vessel might experience low rudder inflow speed facing downstream current as it takes more time to turn the ship heading to align with the target course, as seen in Figure 26(b) and Figure 27. As inland vessels typically reduce speed when navigating confined waterways to prevent additional squat, the relatively low incoming speed due to downstream current further contributes to lower rudder force.

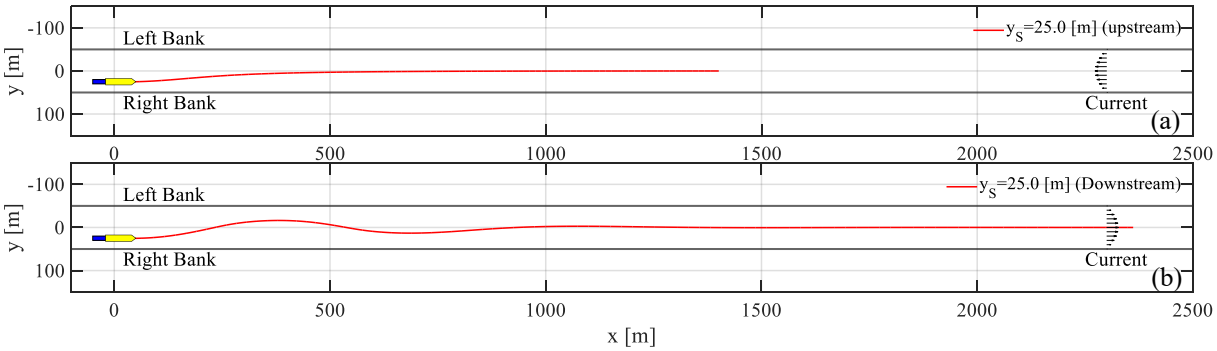

Figure 26. Vessel trajectory for mid-channel course keeping.

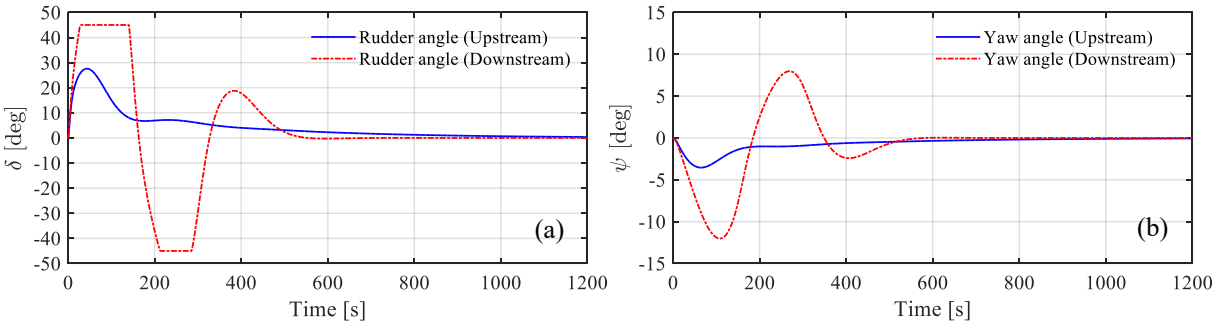

Figure 27. Time histories of the rudder and heading angles for different current directions.

Regarding the second navigation scenario, the rudder control might become challenging due to the increased bank-induced force and moment if the ship sails close to the shore. The simulation result presented in Figure 28 denotes that rudder control cannot converge in the downstream direction because the rudder capacity with the original twin-propeller twin-rudder (TPTR) steering devices is inadequate to counteract the higher hydrodynamic force from the bank.

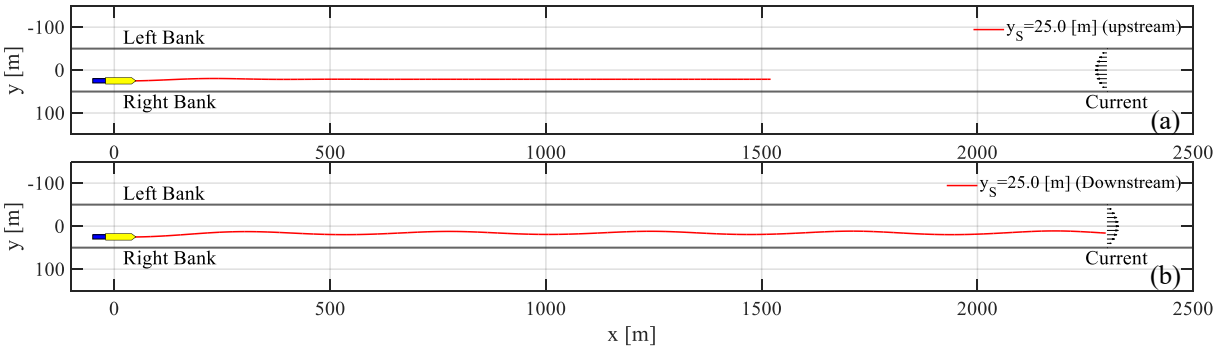

Figure 28. Vessel trajectories for sailing along the bank in TPTR configuration.

An additional analysis was performed by improving the steering units from TPTR to TPQR (a four-propeller configuration), a widely used system in modern European inland vessels. The results in Figure 29 show that the additional rudders effectively address the issue even at low propeller speeds. Compared to the original TPTR configuration, the rudder control converges well for the TPQR system and remains at a constant angle, as seen in Figure 30.

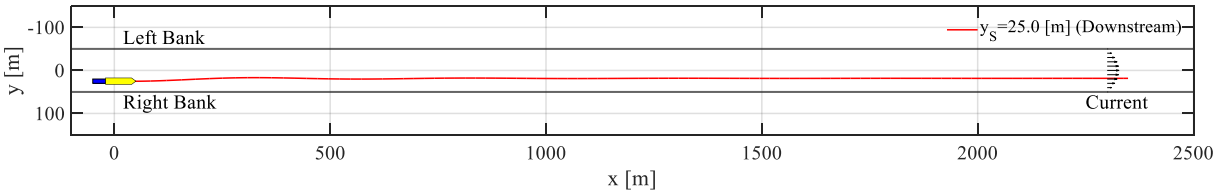

Figure 29. Vessel trajectory using TPQR configuration.

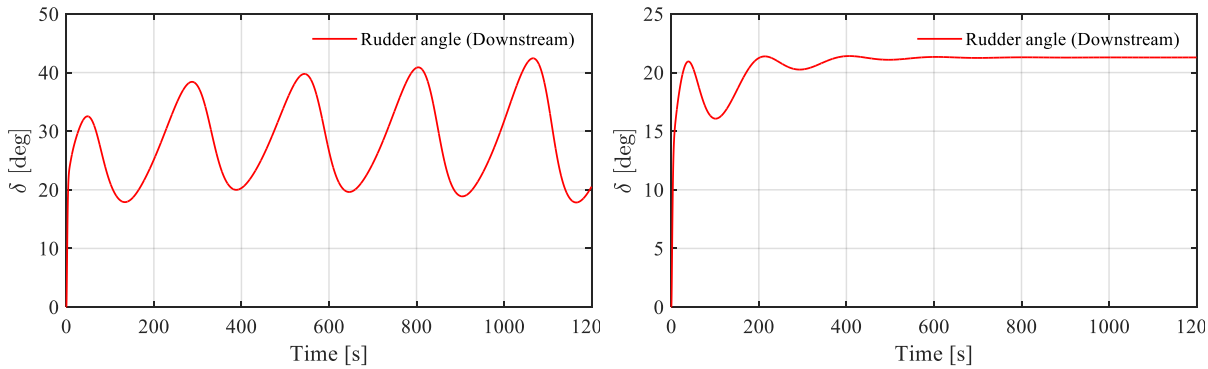

Figure 30. Time histories of rudder control in (left) TPTR and (right) TPQR configurations.

4 Conclusions

To advance the use of autonomous inland vessels for future intelligent waterborne shipping, one of the key challenges is ensuring that these vessels align with environmental sustainability goals, particularly regarding energy efficiency. Achieving this goal requires a holistic system capable of monitoring and optimising overall energy consumption during dynamic operations. This involves the development of an energy prediction method, a ship hydrodynamic and manoeuvring model, and a voyage planning tool for optimising sailing energy. The thesis focuses on the first two aspects, proposing suitable methods specifically for inland vessels by considering the features of waterways, such as limited water depth and constraints on channel width. This section summarises the significant findings from Papers I and II.

Development of ship performance model ShipCLEAN-IWV

Evaluating the energy performance of new vessels is challenging due to insufficient data during the early design stage, especially for these advanced future autonomous vessels. One solution is to develop a generic ship energy system model based on ship physics (white box) that uses empirical formulas to quickly simulate and analyse the ship's energy efficiency. In addition to accuracy and computational efficiency, the model should be easy to implement and modify according to the user's purpose.

Paper I presented the development of a holistic energy system model, ShipCLEAN-IWV, which can capture the impact of inland waterways on a vessel's hydrodynamics and model the overall energy performance with limited input parameters. The model uses the ShipCLEAN (Tillig, 2020) model for seagoing vessels as the baseline, with significant improvements in resistance and propulsion prediction considering the shallow water and bank effects.

It was concluded from verification by experimental data that the proposed ShipCLEAN-IWV model has very good resistance prediction accuracy based solely on empirical methods, with a prediction error of 5.8% for a self-propelled vessel and 8.7% for pusher–barge convoys.

The model's power prediction was verified using full-scale data from the literature. The results indicated that the model also has good accuracy in terms of delivered power (P_D) prediction at most operational conditions, including deep to medium shallow water ($H/T \geq 1.78$). The output value in extremely shallow water conditions ($H/T = 1.2$) still agrees with the reference data within the low ship speed range. However, the difference increases when the ship sails at higher speeds due to the additional wave resistance and, more importantly, the difficulty and complexity of predicting wake and thrust deduction in shallow water conditions. Propeller performance and flow analysis in shallow water are challenges for ship hydrodynamics since measuring the wake field when the ship hull is close to the bottom of the waterway is difficult. Considering the developed model's good performance in most speed and water depth conditions and given that inland vessels do not frequently encounter extremely shallow water, this study does not offer a detailed analysis of the propulsion coefficient in very shallow water.

The case study denotes that the loading conditions have a significant impact on IWVs in decreased water depths. Sailing close to the bank can induce additional power and energy consumption, but this has a minor influence compared to water depth. One of the study's main limitations is that it simplified the waterway cross-section into a rectangular shape. In future studies, arbitrary cross-sections with varying current speeds should be included to better represent actual inland waterways. Additionally, the study only considered longitudinal force; this must be extended into a 3-DoF model in future work to include vessel movement and steering in energy performance analysis.

Manoeuvring model for inland vessels

Energy-efficient route planning also requires a manoeuvring model to predict the ship's steering performance. The vessel's movement must be captured under environmental disturbance for a specific rudder command, and the vessel's states need to be updated for energy performance analysis. The current research on ship manoeuvring primarily focuses on standard commercial vessels in deep water, which may not apply to inland waterways due to significant differences in sailing environment and vessel shape. Therefore, Paper II in this thesis proposed a new manoeuvring model by incorporating additional hydrodynamic impacts (shallow water and bank effects) into the classical MMG model.

A verification study was initially conducted based on experimental measures of a pusher–barge convoy. The simulation results indicated that the turning circles matched well with the literature at 20° and 35° rudder angles. The simulation based only on the bank effect suggested that this effect has a noticeable impact on the ship's course stability in confined waterways. Thus, a rudder controller was developed, and a coupled analysis, including bank and current effects, was performed to investigate the vessel's manoeuvring performance in counteracting these additional disturbances to maintain a predefined course and ensure operational safety.

The manoeuvring model is modular-based and can be easily integrated into the energy system model to investigate the ship's performance in a 3-DoF domain. However, one of the main limitations is that simulations were conducted only in a straight channel with an oncoming current. Thus, future studies must include curved waterways and current fields to capture the nature of actual inland waterways. Furthermore, different control techniques should be evaluated and adopted for complex navigation scenarios, such as manoeuvring in river intersections. The present methods consider only heading as the control objective with a constant propeller speed for maintaining a straight course.

5 Future work

The long-term goal of this research is to develop an integrated system for smart voyage planning of future autonomous inland vessels to improve energy efficiency. This goal requires systematically studying ship hydrodynamics, propulsion systems, route planning, and voyage optimisation. Based on the findings of the present thesis, the focus of future work can be divided into the following topics.

Extension of engine and energy storage system development

The present thesis considers only conventional diesel engines, as most current IWVs use fossil fuels for power generation. To achieve a sustainable perspective and meet the demand for future autonomous vessels, the engine model should be extended to include new technologies, such as hybrid engines, batteries, and fuel cells. This extension will allow the development of a simulation tool for different inland vessel engines to analyse energy consumption comprehensively.

Development of a generic manoeuvring model

The current manoeuvring model still relies on detailed vessel parameters, such as hydrodynamic coefficients, propeller efficiency curves, and rudder inflow parameters. These factors strongly depend on the specific ship type and are thus very sensitive for general applications. In addition, the model only includes a conventional propeller–rudder system, while modern inland vessels are equipped with other steering devices, such as azimuth thrusters, tunnel thrusters, and water jets. Therefore, a generic manoeuvring model must be developed. A database for predicting hydrodynamic coefficients should be built based on measurements or numerical manoeuvring simulation (e.g., virtual captive tests based on CFD) of different inland vessels and investigating the applicability and accuracy of empirical methods, especially for ships in the early design stage with limited parameters.

Voyage planning platform design

A simulation platform should be developed for voyage planning to evaluate the operational energy performance of autonomous inland vessels. This requires implementing and integrating the abovementioned energy prediction model, manoeuvring model, motion control, and future studies regarding waterway generation, and especially the advanced path planning algorithms from research in the AUTOBarge project. The possible interaction with dynamic traffic must be considered as well.

Energy management optimisation

An optimisation study should be conducted during vessel operations, primarily on navigation safety and energy consumption. It should involve engine modes switching, load optimisation, speed and trim adjustment, optimal steering, and collision avoidance (e.g., ensuring operational safety while passing head-on, overtaking other vessels, and passing through locks). In addition, the overall emissions and mission endurance should be evaluated and optimised based on the fuel or engine selection.

6 References

Abkowitz, M. A. (1964). *Lectures on ship hydrodynamics--Steering and manoeuvrability*. Hydro- and Aerodynamics Laboratory, Hydrodynamics Section, Lyngby, Denmark, Report No. Hy-5, Lectures.

Aztjushkov, L. (1968). *Wall effect correction for shallow water model tests*. The North East Coast Institution of Engineers and Shipbuilders, Bolbec Hall, Great Britain, Transactions, *85*(2), Leningrad Shipbuilding Institute, Russia.

Bui, K. Q., & Perera, L. P. (2021). Advanced data analytics for ship performance monitoring under localized operational conditions. *Ocean Engineering*, *235*, 109392. https://doi.org/10.1016/j.oceaneng.2021.109392

Calleya, J. N. (2014). *Ship design decision support for a carbon dioxide constrained future.* Doctoral thesis. University College London.

Clarke, D. (2003). The foundations of steering and manoeuvring. In *Proceedings of the IFAC Conference on Manoeuvering and Control Marine Crafts*, Girona.

Du, P., Ouahsine, A., Sergent, P., & Hu, H. (2020). Resistance and wave characterizations of inland vessels in the fully-confined waterway. *Ocean Engineering*, *210*, 107580. https://doi.org/10.1016/j.oceaneng.2020.107580

Eloot, K., & Vantorre, M. (2011). Ship behaviour in shallow and confined water: an overview of hydrodynamic effects through EFD. *Assessment of stability and control prediction methods for NATO air and sea vehicles*, *20*. NATO. Research and Technology Organisation (RTO).

Epps, B., Chalfant, J., Kimball, R., Techet, A., Flood, K., & Chryssostomidis, C. (2009). OpenProp: An open-source parametric design and analysis tool for propellers. In Proceedings of the 2009 grand challenges in modeling & simulation conference,

European Commission. (2023). *Freight transport statistics - modal split.* Eurostat. https://ec.europa.eu/eurostat/statistics-explained/index.php?title=Freight_transport_statistics_-_modal_split

European Commission. (2018). 2050 long-term strategy. https://climate.ec.europa.eu/eu-action/climate-strategies-targets/2050-long-term-strategy_en

European Commission. (2020). *AUTOBarge: European training and research network on autonomous barges for smart inland shipping.* https://etn-autobarge.eu/

European Environment Agency. (2017). *Specific CO2 emissions per tonne-km and per mode of transport in Europe*. https://www.eea.europa.eu/data-and-maps/daviz/specific-co2-emissions-per-tonne-2#tab-chart_1

Fossen, T. I. (2011). *Handbook of marine craft hydrodynamics and motion control*. John Wiley & Sons.

Friedhoff, B., Hoyer, K., List, S., & Tenzer, M. (2019). Investigation of the nominal and effective propeller inflow for a family of inland waterway vessels. *Ocean Engineering*, *187*, Article 106180. https://doi.org/10.1016/j.oceaneng.2019.106180

Geerts, S., Verwerft, B., Vantorre, M., & Van Rompuy, F. (2010). Improving the efficiency of small inland vessels. In *Proceedings of the 7th European Inland Waterway Navigation Conference, Budapest University of Technology and Economics*, Budapest, Hungary,

Hidouche, S., Guitteyn, M., Linde, F., & Sergent, P. (2015). Ships propulsion: Estimation of specific fuel consumption based on power load factor ratio. In *Proceedings of Hydrodynamics and Simulation Applied to Inland Waterways and Port Approaches*.

Hu, Z. H., Jing, Y. X., Hu, Q. Y., Sen, S., Zhou, T. R., & Osman, M. T. (2019). Prediction of fuel consumption for enroute ship based on machine learning. *IEEE Access*, *7*, 119497–119505. https://doi.org/10.1109/access.2019.2933630

Huang, L. F., Li, Z. Y., Ryan, C., Ringsberg, J. W., Pena, B., Li, M. H., Ding, L., & Thomas, G. (2021). Ship resistance when operating in floating ice floes: Derivation, validation,

and application of an empirical equation. *Marine Structures*, *79*, Article 103057. https://doi.org/10.1016/j.marstruc.2021.103057

Inoue, S., Hirano, M., & Kijima, K. (1981). Hydrodynamic derivatives on ship manoeuvring. *International Shipbuilding Progress*, *28*(321), 112–125.

Islam, H., Soares, C. G., Liu, J., & Wang, X. (2021). Propulsion power prediction for an inland container vessel in open and restricted channel from model and full-scale simulations. *Ocean Engineering*, *229*, Article 108621. https://doi.org/10.1016/j.oceaneng.2021.108621

Karagiannidis, P., & Themelis, N. (2021). Data-driven modelling of ship propulsion and the effect of data pre-processing on the prediction of ship fuel consumption and speed loss. *Ocean Engineering*, *222*, Article 108616. https://doi.org/10.1016/j.oceaneng.2021.108616

Karpov, A. (1946). Calculation of ship resistance in restricted waters. *TRUDY GII*. T. IV, Vol. 2 (in Russian).

Kijima, K., & Nakiri, Y. (1990). Prediction method of ship manoeuvrability in deep and shallow waters. In *Proceedings of the Marine Simulation and Ship Manoeuvrability International Conference*, Tokyo, Japan.

Koh, K., & Yasukawa, H. (2012). Comparison study of a pusher–barge system in shallow water, medium shallow water and deep water conditions. *Ocean Engineering*, *46*, 9–17. https://doi.org/10.1016/j.oceaneng.2012.03.002

Kristensen, H. O., & Lützen, M. (2012). Prediction of resistance and propulsion power of ships. *Clean Shipping Currents*, *1*(6), 1–52.

Kulczyk, J. (1995). Propeller–hull interaction in inland navigation vessel. *Transactions on the Built Environment*, *11*, 73–89. https://www.scopus.com/inward/record.uri?eid=2-s2.0-85017473910&partnerID=40&md5=847c24d3b39a9d51dd63a4952ad7f4df

Kulczyk, J., & Tabaczek, T. (2014). Coefficients of propeller–hull interaction in propulsion system of inland waterway vessels with stern tunnels. *TransNav: International Journal on Marine Navigation and Safety of Sea Transportation*, *8*(3), 377–384.

Lackenby, H. (1963). The effect of shallow water on ship speed. *Shipbuilder and Marine Engineer*, *70*, 446–450.

Landweber, L. (1939). *Tests of a model in restricted channels*. David Taylor Model Basin, Washington, D.C.

Lang, X., Wu, D., & Mao, W. G. (2022). Comparison of supervised machine learning methods to predict ship propulsion power at sea. *Ocean Engineering*, *245*, Article 110387. https://doi.org/10.1016/j.oceaneng.2021.110387

Lataire, E., Vantorre, M., & Delefortrie, G. (2018). The influence of the ship's speed and distance to an arbitrarily shaped bank on bank effects. *Journal of Offshore Mechanics and Arctic Engineering*, *140*(2), 021304. https://doi.org/10.1115/1.4038804

Lataire, E., Vantorre, M., & Eloot, K. (2009). Systematic model tests on ship–bank interaction effects. In *Proceedings of the International Conference on Ship Manoeuvring in Shallow and Confined Water: Bank Effects* (pp. 9–22).

Linde, F. (2017). *3D modelling of ship resistance in restricted waterways and application to an inland eco-driving prototype.* Université de Technologie de Compiègne.

Linde, F., Ouahsine, A., Huybrechts, N., & Sergent, P. (2017). Three-dimensional numerical simulation of ship resistance in restricted waterways: Effect of ship sinkage and channel restriction. *Journal of Waterway Port Coastal and Ocean Engineering*, *143*(1), Article 06016003. https://doi.org/10.1061/(asce)ww.1943-5460.0000353

Liu, J., Hekkenberg, R., Quadvlieg, F., Hopman, H., & Zhao, B. (2017). An integrated empirical manoeuvring model for inland vessels. *Ocean Engineering*, *137*, 287–308. https://doi.org/10.1016/j.oceaneng.2017.04.008

Liu, J., Hekkenberg, R., Rotteveel, E., & Hopman, H. (2015). Literature review on evaluation and prediction methods of inland vessel manoeuvrability. *Ocean Engineering*, *106*, 458–471. https://doi.org/10.1016/j.oceaneng.2015.07.021

Lu, R. H., Turan, O., Boulougouris, E., Banks, C., & Incecik, A. (2015). A semi-empirical ship operational performance prediction model for voyage optimization towards energy efficient shipping. *Ocean Engineering*, *110*, 18–28. https://doi.org/10.1016/j.oceaneng.2015.07.042

Mermiris, D., Vassalos, D., Dodworth, K., Sfakianakis, D., & Mermiris, G. (2011). Dynamic energy modelling – A new approach to energy efficiency and cost-effectiveness in shipping operations. In *Proceedings of the Low Carbon Shipping Conference*.

Millward, A. (1989). The effect of water depth on hull form factor. *International Shipbuilding Progress*, *36*(407).

Mucha, P., Dettmann, T., Ferrari, V., & el Moctar, O. (2019). Experimental investigation of free-running ship manoeuvers under extreme shallow water conditions. *Applied Ocean Research*, *83*, 155–162. https://doi.org/10.1016/j.apor.2018.09.008

Mucha, P., el Moctar, O., Dettmann, T., & Tenzer, M. (2017). Inland waterway ship test case for resistance and propulsion prediction in shallow water. *Ship Technology Research*, *64*(2), 106–113. https://doi.org/10.1080/09377255.2017.1349723

Mucha, P., el Moctar, O., Dettmann, T., & Tenzer, M. (2018). An experimental study on the effect of confined water on resistance and propulsion of an inland waterway ship. *Ocean Engineering*, *167*, 11–22. https://doi.org/10.1016/j.oceaneng.2018.08.009

Nomoto, K., Taguchi, T., Honda, K., & Hirano, S. (1957). On the steering qualities of ships. *International Shipbuilding Progress*, *4*(35), 354–370.

Norrbin, N. H. (1977). Theory and observation on the use of a mathematical model for ship maneuvering in deep and confined water. In *Proceedings of the 8th Symposium on Naval Hydrodynamics*.

Ogawa, A., & Kasai, H. (1978). On the mathematical model of manoeuvring motion of ships. *International Shipbuilding Progress*, *25*(292), 306–319.

Parkes, A. I., Sobey, A. J., & Hudson, D. A. (2018). Physics-based shaft power prediction for large merchant ships using neural networks. *Ocean Engineering*, *166*, 92–104. https://doi.org/10.1016/j.oceaneng.2018.07.060

Pompée, P.-J. (2015). About modelling inland vessels resistance and propulsion and interaction vessel-waterway key parameters driving restricted/shallow water effects. In *Proceedings of Smart Rivers 2015*, Buenos Aires, Argentina, Paper 180.

Raven, H. (2012). A computational study of shallow-water effects on ship viscous resistance. In *Proceedings of the 29th Symposium on Naval Hydrodynamics*, Gothenburg, Sweden.

Raven, H. (2016). A new correction procedure for shallow-water effects in ship speed trials. In *Proceedings of the 2016 PRADS Conference*, Copenhagen, Denmark.

Rijkswaterstaat. (2020). *Waterway guidelines 2020.* Directorate-General for Public Works and Water Management, Rijkswaterstaat.

Rotteveel, E., Hekkenberg, R., & van der Ploeg, A. (2017). Inland ship stern optimization in shallow water. *Ocean Engineering*, *141*, 555–569. https://doi.org/10.1016/j.oceaneng.2017.06.028

Schlichting, O. (1934). Ship resistance in water of limited depth-resistance of sea-going vessels in shallow water. *Jahrbuch der STG*, *35*, 127–148.

Schneekluth, H., & Bertram, V. (1998). *Ship design for efficiency and economy* (Vol. 218). Butterworth-Heinemann Oxford.

Sutulo, S., & Soares, C. G. (2014). An algorithm for offline identification of ship manoeuvring mathematical models from free-running tests. *Ocean Engineering*, *79*, 10–25. https://doi.org/10.1016/j.oceaneng.2014.01.007

Tillig, F. (2020). *Simulation model of a ship's energy performance and transportation costs*. Chalmers Tekniska Hogskola (Sweden).
Tillig, F., Ringsberg, J., Mao, W., & Ramne, B. (2017). A generic energy systems model for efficient ship design and operation. In *Proceedings of the Institution of Mechanical Engineers, Part M: Journal of Engineering for the Maritime Environment*, *231*(2), 649–666. https://doi.org/10.1177/1475090216680672
Tillig, F., & Ringsberg, J. W. (2019). A 4 DOF simulation model developed for fuel consumption prediction of ships at sea. *Ships and Offshore Structures*, *14*(sup1), 112–120. https://doi.org/10.1080/17445302.2018.1559912
Tillig, F., Ringsberg, J. W., Mao, W., & Ramne, B. (2018). Analysis of uncertainties in the prediction of ships' fuel consumption–from early design to operation conditions. *Ships and Offshore Structures*, *13*(sup1), 13–24. https://doi.org/10.1080/17445302.2018.1425519
Vantorre, M. (2003). Review of practical methods for assessing shallow and restricted water effects. In *Proceedings of the International Conference on Marine Simulation and Ship Maneuverability (MARSIM 2003)*, Kanazawa, Japan: International Marine Simulator Forum.
Vantorre, M., Delefortrie, G., Eloot, K., & Laforce, E. (2003). Experimental investigation of ship–bank interaction forces. In *Proceedings of MARSIM '03*, Kanazawa, Japan.
Vantorre, M., Eloot, K., Delefortrie, G., Lataire, E., Candries, M., & Verwilligen, J. (2017). Maneuvering in shallow and confined water. In *The Encyclopedia of Marine Offshore Engineering* (pp. 1–17). https://doi.org/10.1002/9781118476406.emoe006
Yamazaki, D., Ikeshima, D., Sosa, J., Bates, P. D., Allen, G. H., & Pavelsky, T. M. (2019). MERIT Hydro: A high-resolution global hydrography map based on latest topography dataset. *Water Resources Research*, *55*(6), 5053–5073. https://doi.org/10.1029/2019WR024873
Yasukawa, H., & Yoshimura, Y. (2015). Introduction of MMG standard method for ship maneuvering predictions. *Journal of Marine Science and Technology*, *20*, 37–52.
Yoshimura, Y. (1986). Mathematical model for the manoeuvring ship motion in shallow water. *Journal of the Kansai Society of Naval Architects* (200).
Zeng, Q. (2019). *A method to improve the prediction of ship resistance in shallow water*. Doctoral thesis. Delft University of Technology.
Zeng, Q., Hekkenberg, R., Thill, C., & Hopman, H. (2020). Scale effects on the wave-making resistance of ships sailing in shallow water. *Ocean Engineering*, *212*, 107654. https://doi.org/10.1016/j.oceaneng.2020.107654
Zeng, Q., Thill, C., & Hekkenberg, R. (2018). A benchmark test of ship resistance in extremely shallow water. In *Progress in Maritime Technology and Engineering* (pp. 221–229). CRC Press.
Zeng, Q. S., Hekkenberg, R., & Thill, C. (2019). On the viscous resistance of ships sailing in shallow water. *Ocean Engineering*, *190*, 106434. https://doi.org/10.1016/j.oceaneng.2019.106434
Zentari, L., el Mocta, O., Lassen, J., Hallmann, R., & Schellin, T. E. (2022). Experimental and numerical investigation of shallow water effects on resistance and propulsion of coupled pusher–barge convoys. *Applied Ocean Research*, *121*, 103048. https://doi.org/10.1016/j.apor.2022.103048
Zentari, L., Tödter, S., el Moctar, O., Neugebauer, J., & Schellin, T. E. (2023). Experimental and numerical investigation of the gap flow between a pusher and a barge in deep and shallow water. *Applied Ocean Research*, *132*, 103466. https://doi.org/10.1016/j.apor.2023.103466

Zou, L., & Larsson, L. (2013). Computational fluid dynamics (CFD) prediction of bank effects including verification and validation. *Journal of Marine Science and Technology*, *18*(3), 310–323. https://doi.org/10.1007/s00773-012-0209-7